The Effect of pH and Solvent in the Photophysics of Thymine

by

Ali Mohamoud Abdallah

A Thesis Presented to the

FACULTY OF THE COLLEGE OF GRADUATE STUDIES

KING FAHD UNIVERSITY OF PETROLEUM & MINERALS

DHAHRAN, SAUDI ARABIA

In Partial Fulfillment of the
Requirements for the Degree of

MASTER OF SCIENCE

In

CHEMISTRY

December, 1996

The Effect of pH and Solvent on the Photophysics of Thymine

BY

ALI MOHAMOUD ABDALLAH

A Thesis Presented to the

FACULTY OF THE COLLEGE OF GRADUATE STUDIES

KING FAHD UNIVERSITY OF PETROLEUM & MINERALS

DHAHRAN, SAUDI ARABIA

In Partial Fulfillment of the
Requirements for the Degree of

MASTER OF SCIENCE

In

CHEMISTRY

December 1996

UMI
300 North Zeeb Road
Ann Arbor, MI 48103

KING FAHD UNIVERSITY OF PETROLEUM AND MINERALS
DHAHRAN, SAUDI ARABIA

COLLEGE OF GRADUATE STUDIES

This thesis, written by **Ali Mohamoud Abdallah** under the direction of his Thesis Advisor and approved by his Thesis Committee, has been presented to and accepted by the Dean of the College of Graduate Studies, in partial fulfillment of the requirements for the degree of **MASTER OF SCIENCE** in **Chemistry.**

Thesis Committee:

A. Suwaiyan

Prof. Abdul-Aziz A. Al-Suwaiyan
Thesis Advisor

Prof. Uwe Karl Albert Klein
Member

M. A. Morsy

Dr. Mohamed Ali Morsy
Member

Dr. Abdulrahman A. Al-Arfaj
Department Chairman

Dr. Abdullah M. Al-Shehri
Dean, College of Graduate Studies

Date: 29-12-96

To My Parents

ACKNOWLEDGEMENT

Acknowledgement is due to King Fahd University of Petroleum and Minerals for support of this research.

I would like to express my profound gratitude to my advisor, Prof. Abdul-Aziz A. Al-Suwaiyan without whom this work would not have been possible. I am also indebted to the other members of my Thesis Committee, Prof. Uwe Karl A. Klein and Dr. Mohamed Ali Morsy for their valuable discussions.

I would like to express my sincere thanks to Dr. Abdulrahman A. Al-Arfaj, Chairman, Chemistry Department, KFUPM, for his support and encouragement. I am also grateful to Prof. Fida F. Al-Adel, Manager, Division II, Research Institute, KFUPM, for kindly allowing me to make use of the laser system in the Laser Research Laboratory. My thanks also go to Mr. Azam Baig for optimizing the laser system.

Last but not least, I wish to express my thanks and appreciation to faculty and staff members of Chemistry Department for their help and consideration throughout this research.

TABLE OF CONTENTS

Page

LIST OF TABLES

LIST OF FIGURES

THESIS ABSTRACT

Full Name of Student	:	Ali Mohamoud Abdallah
Title of Study	:	The Effect of pH and Solvent on the Photophysics of Thymine
Major Field	:	Physical Chemistry
Date of Degree	:	December 1996

The effect of pH and various alcohol-water mixtures on the electronic spectra and excited state dynamics of thymine, one of the DNA constituents, have been investigated. A mode-locked Nd:YAG laser in combination with a cavity-dumped synchronously-pumped dye laser is used as a source of excitation. Fluorescence decay and time-resolved spectra were recorded with picosecond photon counting spectrometer. Steady-state fluorescence spectra as well as ultraviolet absorption spectra were also recorded.

Fluorescence spectra of thymine in aqueous solutions where thymine exists in the neutral form have been found to vary in shape as the excitation wavelength is increased. This change in shape is explained by the presence of another tautomer beside the predominant diketo tautomer of thymine. This minor tautomer is believed to be 5-methyl-2-hydoxy-4(3H)-pyrimidinone or the keto-enol tautomer. Lifetime analysis of fluorescence decays support this explanation where a biexponential decay with lifetimes of around 0.7 and 4 ns is observed for the neutral form of thymine. Time-resolved spectra are in accordance with this explanation.

Fluorescence lifetimes of thymine do not vary in methanol-water and ethanol-water mixtures. While the lifetime of the keto-enol tautomer is found to vary with viscosities of the 1-propanol-water mixtures. This is explained by solvent-solvent and solute-solvent interaction. According to the steady-state and time-resolved fluorescence spectra in the various alcohol-water mixtures, thymine does not undergo a pK_a shift in the excited state.

MASTER OF SCIENCE DEGREE

KING FAHD UNIVERSITY OF PETROLEUM AND MINERALS
Dhahran, Saudi Arabia

December 1996

خلاصة الرسالة

اسم الطالب الكامل : علي محمود عبدالله

عنـــوان الرسالـــــة : تأثير الرقم الهيدروجيني والمذيب على الفيزياء الضوئية لمركب الشايين .

التخصـــــــــص : كيمياء فيزيائية

تاريـخ الشهـــــادة : ديسمبر ١٩٩٦م

تم استقصاء تأثير الرقم الهيدروجيني ومخاليط متعددة من الماء والكحولات على الأطياف الإلكترونية وديناميكية الحالة المثارة لمركب الشايين الذي يدخل في تكوين الحامض الخلوي د. ن. أ.

واستخدم نظام الطور المغلق لموجات الليزر لإثارة صبغ ليزر ذي تفريغ فجوي بشكل متزامن الذي بدوره استخدم لإثارة المركب . وقد تم جمع منحنيات تلاشي الفلورية ، وأطياف الزمن التحللي بواسطة مطياف البيكوسكند . كما تم تسجيل أطياف الفلورية في الحالة المستقرة وأطياف الامتصاص أيضاً .

وجد أن أطياف الفلورية في الحالة المستقرة للشايين المتعادل في محاليل الماء تعتمد على الأطوال الموجية المستخدمة للإثارة. عزي هذا التغير في شكل أطياف الفلورية بوجود مماثل كيماوي آخر بجانب المماثل الكيماوي الغالب لمركب الشايين . يعتقد أن هذا المماثل هو ٥ - ميثايل - ٢ - هيدروكسي - ٤ (H ٣) - بريميدونون أو مماثل الكيتوراينول . وأيدت نتائج تلاشي الفورية هذا الاعتبار حيث وجد أن منحنيات تلاشي الفلورية لمركب الشايين المتعادل ثنائية الاس بقيمة ٧ر٠ و ٤ نانوسكند . كما أن أطياف الزمن التحللي تلائم هذا الشرح .

لوحظ أن أزمان تلاشي الفلورية للشايين لاتتغير باستعمال مخاليط مختلفة من الماء والميثانول والماء والايثانول بينما وجد أن أزمان تلاشي الفلورية تتغير بتغير معامل اللزوجة في مخاليط مختلفة من الماء و ١ - بروبانول . عزي هذا إلى تفاعل تبادلي بين المذيبين من جهة والمذيب والمذاب من جهة أخرى كما وجد أيضاً أن ثابت الحموضة لمركب الشايين لايتغير في الحالة المثارة .

درجة الماجستير في العلوم

جامعة الملك فهد للبترول والمعادن

الظهران ، المملكة العربية السعودية

ديسمبر ١٩٩٦

CHAPTER I

INTRODUCTION

CHAPTER I

INTRODUCTION

1.1 Objectives and Scope of this Research

The excited electronic structure of the DNA bases has been of considerable interest[1] to help understand the photochemistry and photobiology of DNA, and fluorescence is a major tool for investigating the behavior of excited states. Hauswirth and Daniels[2] were the first to investigate the fluorescence of thymine in aqueous solution at room temperature. The excitation spectrum of thymine reported by Hauswirth and Daniels[2] exhibited a significant deviation from the corresponding absorption spectrum. They explained their results in terms of (a) the presence of two overlapping $n\pi^*$ and $\pi\pi^*$, where only one of them will fluoresce, (b) emission from a minor tautomer (2, 4-dienol), or (c) kinetics of competing deactivation processes. Because of excitation spectrum deviation, Hauswirth and Daniels concluded that the fluorescence quantum yield is not constant over the absorption band. This conclusion has been reached, as well, by Wilson et al[3]. However, Vigny and Duquesne[4] and R.S. Becker and G. Kogan[5] indicated that there is no excitation wavelength dependence for the fluorescence quantum yield.

Since the first room temperature fluorescence reported by Hauswirth and Daniels[2], a lot of theoretical and experimental studies have been published on the structure and electronic spectra of uracil, thymine and their derivatives[1,6,7]. However, contradictory conclusions were often reported on the basis of these studies. Morgan and Daniels[8] investigated the polarization excitation spectrum of thymine fluorescence in neutral aqueous solutions. They suggested that fluorescence polarization of thymine is dependent on the excitation wavelength. They attributed the dramatic depolarization at the red edge of the absorption band (280 - 290 nm) to a weak out-of-plane absorption and proposed the presence of a hidden $n\pi^*$ transition. On the other hand, P. Callis[9] reported that the fluorescence polarization is independent of the excitation wavelength even at the red edge of the absorption band (290 nm). Subsequent work by Williams, Renn and Callis[10] rantionalized the difference between their findings and those of Morgan and Daniels on the basis of the pH of the solutions used by the two groups. They pointed out that the contribution from the anion in the case of Morgan and Daniels experiment was the mere reason for the depolarization observed.

Recent studies conducted by Fujii and coworkers[6,11] on the fluorescence excitation and dispersed fluorescence spectra of jet-cooled uracil, thymine and their derivatives have found that the vibrational spacings seen in these emission spectra agreed very well

with the ground-state vibrational frequencies in the IR and Raman spectra of the 2, 4-diketo tautomer of uracil.

Brady, Peteunu and Levy[12], however, monitored the photoionization mass spectrum of a uracil molecular beam and attributed the sharp spectrum reported by Fujii et al.[11] to an impurity formed in the oven with a higher molecular weight than uracil.

According to Baraldi et al.[7] and Callis et al.[10] it is believed that the emission in aqueous solution is due to the $\pi\pi^*$ transition. However, using a multimode vibrational analysis of the resonance Raman excitation profile of Uridine 5-monophasphate, P. Turpin and W. Pet[13] suggested that the emission is from a lower-lying state carrying negligible oscillator strength to the ground state and different from the strong $\pi\pi^*$ transition.

Very recently, Suwaiyan, Morsy and Odah[14] have studied room temperature fluorescence of 5-chlorouracil. According to their study, the shape of the fluorescence spectrum is found to change when the excitation wavelength is varied. By using picosecond laser pulses they reported a biexponential fluorescence decay. They related the fluorescence excitation wavelength dependence and the non-exponential decay to the presence of at least

one tautomer beside the predominant tautomer namely; the diketo tautomer.

The aforementioned discussion shows that our understanding of excited state structure and dynamics of DNA basis remains fragmented and incomplete though work over the last three decades has yielded considerable progress.

It is quite clear that the photophysics of DNA bases has to be explored further. With the advent of picosecond pulsed lasers, direct dynamic determination of fluorescence lifetimes in the picosecond regime and time evolution of emission have been realized. It is our belief that using such technique may shed some light on the problem at hand.

Therefore, the objective of this work is to study the photophysical behavior of thymine under different environmental conditions. At various pH, the effect of excitation wavelength on the shape of steady state fluorescence spectra was investigated. Moreover, direct determination of fluorescence lifetimes using picosecond laser pulses was made. The second part was concerned with the effect of methanol-water, ethanol-water and 1-propanol-water mixtures on the fluorescence decay of thymine. Finally, time-resolved spectra of thymine were collected in aqueous solutions of different pH and in various alcohol-water mixtures.

1.2 Theory

1.2.1 Source of Complication in the Study of Thymine[1]

The structures of the expected six tautomers of thymine in Figure 1.1 show the source of problems not encountered in the study of hydrocarbons, even those having many more atoms. A close look at the predominant tautomer (diketo tautomer, I) reveals the follows:

1) It is isoelectronic to nonexistent hydrocarbons (di-and trianions) excluding any correlations with well understood systems.
2) The existence of many nonbonded pairs and mobile protons paves the way for tautomeric equilibria, both real and imagined. Moreover, nonbonding electrons presence suggest the presence of low-lying $n\pi^*$ states.
3) The low symmetry associated with this molecule which does not go beyond the single reflection plane makes theoretical efforts rather complicated.

1.2.2 Absorption Spectra of Thymine and Uracil

The absorption spectra in solution shows three broad and unstructured maxima in the energy range up to 7ev (177 nm). These are located at about 260, 205 and 177 nm and each has an oscillator strength of about 0.2 (Figure 1.2). Five transitions are

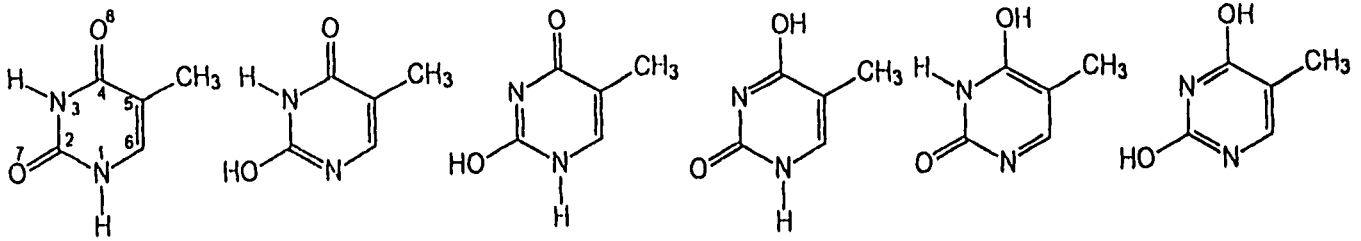

Figure 1.1: Tautomers of Thymine.

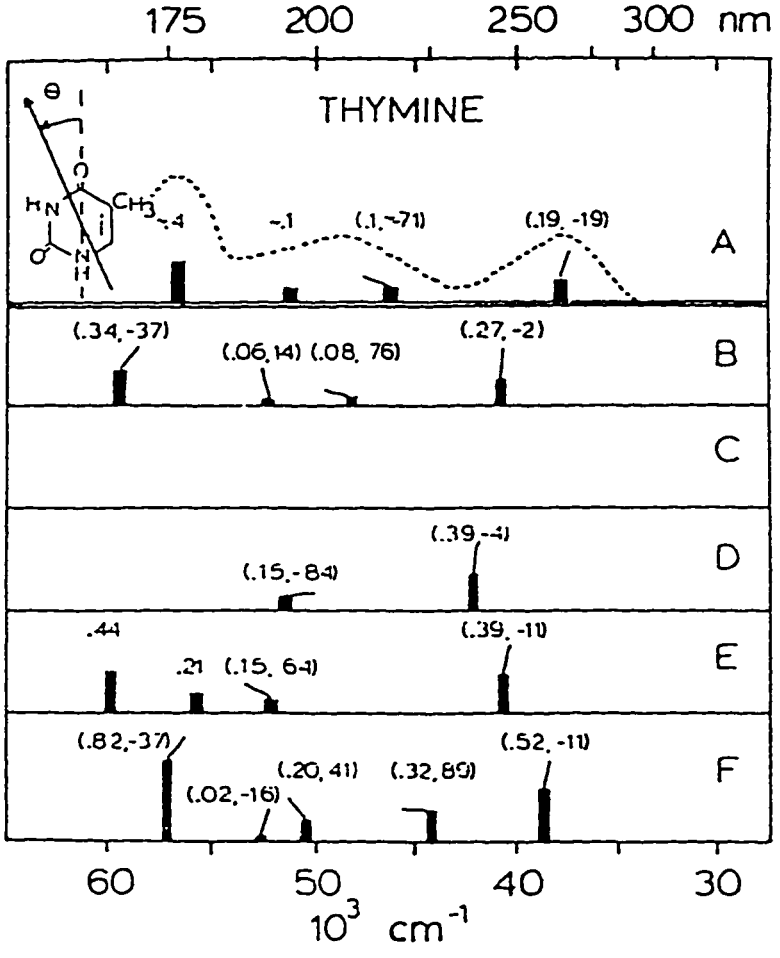

Figure 1.2: Calculated and experimental absorption spectra and polarization for thymine (A) Experimental: θ and f values at 265 for 1-methylthymine. (B-F) calculated, (adapted from Ref. 1).

generally predicted by theory[1]. Most calculations insist on a large gap (6000 - 11,000 cm^{-1}) between the first two $\pi\pi^*$ bands[1]. The first band for thymine is slightly red shifted relative to uracil. This is because substitution of a hydrogen atom with a-methyl group in uracil destabilizes the highest occupied molecular orbital (HOMO). Such a behavior is due to the fact that this orbital is localized on the atoms N1C5C6 so that a particularly effective hyperconjugation is established only when hydrogens in these positions are replaced[15,16].

According to ab initio multireference configuration interaction (MRCI) and random-phase approximation (RPA), the intensity of the first band is due to a single intense $\pi\pi^*$ transition[17]. This is in agreement with the results of all semiempirical studies[18-20] reported which predicts a single intense $\pi\pi^*$ transition. Most polarized absorption[21] and reflection[22] experiments on uracil derivatives have interpreted the 260 nm band as a single $\pi\pi^*$ transition and agree that the polarization direction is close to 0^o for uracil and -20^o for thymine. Both linear dichroism spectrum of uracil and the fluorescence polarization spectrum of thymidine monophosphate reveal no evidence of an additional transition of significant oscillator strength in the first band[17].

1.2.3 Polarized Fluorescence

1.2.3.1 Steady-State Anisotropy[23,24]

When a fluoroscent sample is excited with a polarized light, only those fluorophore molecules whose absorption transition dipole is parallel to the electric vector of the incident radiation are excited. This selective excitation of a partially oriented population of fluorophores results in a partially polarized fluorescence emission. The transition moments for absorption and emission have a fixed orientations within each fluorophore, and the relative angle between these moments determines the maximum polarization observed. In steady-state polarized fluorescence, the observed polarization is measured in terms of anisotrophy (γ_o) which is defined by:

$$\gamma_o = \frac{I_{11} - I_{\perp}}{I_{11} + 2I_{\perp}} \qquad (1.1)$$

where I_{11} , $I_{\perp}$ are observed intensities in parallel and perpendicular to the direction of the polarized excitation respectively.

Generally, the absorption and emission dipoles of a flurophore are not colinear. Instead, they are oriented at an angle within the plane of the flurophore. It is noteworthy that the electric dipole of the fluorophore need not be precisely aligned with the Z axis to absorb light polarized along this axis. The probability of absorption is proportional to the $\cos^2\theta$, where θ is the angle the absorption

dipole makes with the Z axis. Therefore, excitation with polarized light results in a population of excited fluorophores which are symmetrically distributed around the Z axis. This phenomenon is called photoselection. Hence the steady-state anisotropy in a vetrified dilute solution is a product of the loss of anisotropy due to photoselection (2/5), and that due to the angular displacement of the dipoles. Therefore,

$$\gamma_o = \frac{2}{5}\left(\frac{3\cos^2\alpha - 1}{2}\right) \qquad (1.2)$$

1.2.3.2 Steady-State Polarized Fluorescence of Thymine

Thymine exhibits very high fluorescence anisotropy in neutral aqueous solution. Value as high as 0.35, which virtually approaches the ideal limit of 0.4, has been reported[8-10]. This value can be attained only if the emitting transition moment is essentially parallel to the absorbing moment.

Callis and coworkers[10] have reported that the anisotropy is independent of the excitation wavelength in the region of 240 to 290 nm for thymine in a pH5 solution.

Morgan and Daniels[8] have measured the polarization excitation spectrum for thymine in aqueous solution at 300K from 240 to 296 nm. They observed that the anisotropy is found to be essentially constant across most of the absorption band and a dramatic depolarization is observed at the red edge of the absorption band.

1.2.4 Fluorescence Decays

1.2.4.1 Causes of a Complex Decay[25,26]

Nonexponential fluorescence decays can arise in many different ways, including (1) simultaneous excitation of two or more different compounds having different fluorescence lifetimes; (2) excitation of molecules of the same compound situated in different environments; (3) presence of multiple molecular conformations; (4) quenching and energy-transfer phenomena; (5) fast excited-state chemical reaction (proton transfer; exciplex or excimer formation).

1.2.4.2 Fluorescence Decay of 5-Chlorouracil[14]

Suwaiyan, Morsy and Odah have investigated the fluorescence decay of 5-chlorouracil in aqueous solutions of different pH for the first time. According to their study, the fluorescence decay is non-

exponential for both the neutral and anionic forms of 5-chlorouracil. In pH 4 solution, for example, where only the neutral form exists, a biexponential decay is observed for the fluorescence with lifetimes of 0.67 and 3.19 ns. A high normalized preexponential factor ($a_i/\Sigma a_i$), i.e., 0.84 is observed for the short lifetime at 360 nm. Upon increasing the emission wavelength to 400 nm, the relative contribution of the short lifetime drops to 0.67 accompanied by a substantial increase in the relative quantum yield ($Q_i = a_i \tau_i/\Sigma a_i \tau_i$) of the longer lifetime. In pH 10 solution, where 5-chlorouracil exists in the anionic form, a biexponential decay is also observed with lifetimes of about 0.2 and 3.4 ns. By taking into account the excitation wavelength dependence of the steady-state fluorescence spectra of 5-chlorouracil, the biexponential decay observed in both neutral and anionic forms of 5-chlorouracil is attributed to the presence of two tautomers in the ground state. Accordingly, in the aqueous solution of pH 4, the short lifetime of 0.67 ns is assigned to the diketo tautomer (I, Figure 1.1) while the longer lifetime of 3.19 ns is attributed to the decay of the keto-enol tautomer (II, Figure 1.1). On the other hand, the biexponential decay of 5-chlorouracil in pH 10 is due to the respective fluorescence decay anions of the diketo and keto-enol tautomers. Therefore, the lifetimes of 0.2 and 3.4 ns are assigned to the fluorescence decay of the diketo and keto-enol anions respectively. The afore-mentioned argument is further confirmed by time-resolved spectra of 5-chlorouracil. In pH 4 solution, for example, two time-resolved bands representing

emission from different tautomers are observed. Fluorescence at shorter times with maximum around 330 nm is attributed to the diketo tautomer whereas fluorescence at longer times with maximum around 400 nm is attributed to the keto-enol tautomer.

CHAPTER II

EXPERIMENTAL

CHAPTER II

INTRODUCTION

2. Experimental

2.1 Materials

Thymine was purchased from Fluka AG, and recrystallized from triply deionized water followed by sublimation under vacuum. To judge the purity of the sample, the fluorescence spectrum of the sample was compared with fluorescence spectra reported by Callis et al.[9] and found to be almost identical.

As far as solvents are concerned, triply deionized water was used throughout the experiments. Spectral grade methanol, ethanol and 1-propanol (puriss) from Fluka were used. Ready-made Fluka buffers at different pH were used to control the pH of the solutions. These solvents were used without any further purification.

2.2 Preparation of Solutions

To study the effect of pH on absorption steady-state fluorescence and fluorescence decays of thymine, standard buffer

solutions (pH1 to pH10) from Fluka were used. To extend the study into the alkaline medium, solutions with pH 12.0 and 13.0 were prepared from NaOH and $CaCl_2$ solutions.

Alchohol-water mixtures with water volume percentage of 0% 10%, 20%, 30%, 40%, 50%, 60%, 70%, 80%, 90%, and 100% were prepared. In alcohol-water mixtures as well as aqueous solutions the concentration of thymine was kept at 1.00×10^{-4} M.

2.3 Absorption and Steady-State Fluorescence Measurements

Absorption spectra were recorded by a Lambda 5 UV/VIS spectrophotometer. Fluorescence spectra were recorded with an SPF-500 spectrofluorometer from SLM Instruments Inc. and corrected for lamp intensity and photomultiplier sensitivity.

2.4. Lifetime Measurement

Samples were excited at 295 nm with a frequency doubled, cavity dumped, mode-locked synchronously pumped dye laser system. In this configuration an Nd: YAG laser (Spectra-Physics Model 3800) was mode locked using an acoustooptic device (Spectra-

Physics Model 451) providing pulses of around 150 ps fwhm (full width at half maximum intensity), at a repetition rate of 82 MHz, and with average power of 500 mW. These pulses were used to excite Rhodamine 6G dye in ethylene glycol in a jet stream dye laser (Spectra-Physics Model 375). To allow total system relaxation between excitation events, an acoustooptic cavity dumper (Spetra-Physics Model 344) was used at 4 MHz. Frequency doubling of the dye laser output was achieved with angle-tuned frequency doubler (Spetra-Physics Model 390). For stability the laser system was mounted on a mechanically isolated optical table (Newport Research Corp.).

The sample was contained in a 1-cm^2 quartz cell. Fluorescence was monitored at a right angle to the excitation path through an emission monochromator having a symmetrical Czerny-Turner optical design by a fast photomultiplier (Philips XP2020Q) mounted in an insulated housing. A multichannel analyzer (Ortec Model 5500) operating in pulse height analysis mode was employed for transfer of data to a PDP 11/23 computer for analysis. Curve fitting deconvolution software supplied by Applied Photophysics was used. Measurements were done at room temperature around 21.5 ^oC. The scattered excitation function was first collected followed by the sample fluorescence decay.

A schematic diagram of the time-resolved fluorescence spectrometer is shown in Figure 2.1

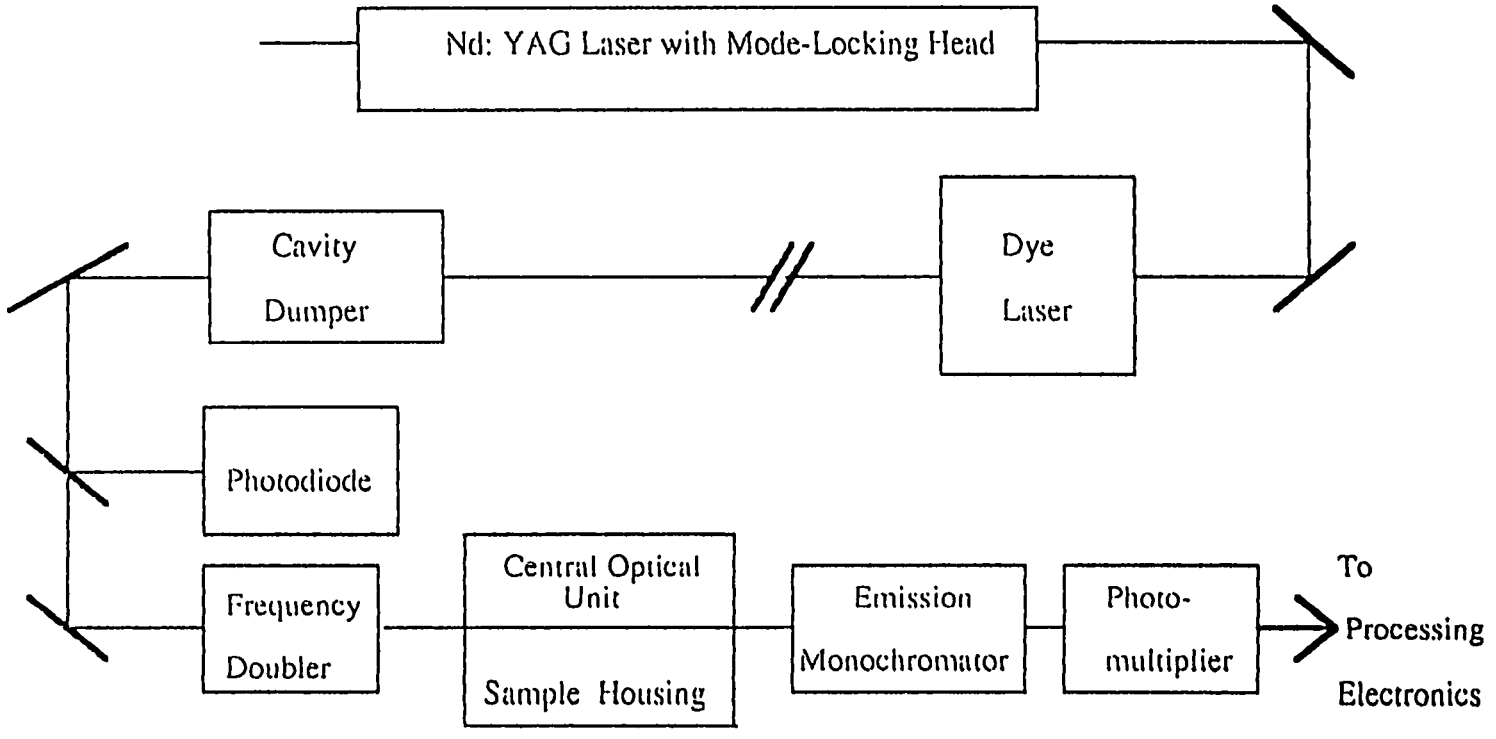

Figure 2.1: Block diagram of a time-resolved fluorescence spectrometer.

2.5 Time-Resolved Spectra

Emitted photons are counted as a function of wavelength and time after excitation. Only photons emitted during a selected time window are recorded in the current channel of the MCA. The MCA is operated in multichannel scaling mode, where each channel corresponds to one wavelength, and the current channel location is incremented in synchrony with the scanning of the emission monochromator.

2.6 Time-Correlated Single Photon Counting Technique

The time evolution of fluorescence, on a time-scale from hundreds of picoseconds to tens of nanoseconds, can be measured by a variety of techniques, but the one which has become the most popular over the last 20 years is time-correlated single photon counting. The level of sophistication accompanying this technique has developed rapidly. The method relies on the basic concept that the probability distribution for emission of a single-photon following excitation gives the actual intensity against time distribution of all photons emitted, thus by sampling the time of single-photon emission following a large number of excitation pulses, the probability distribution is created.

2.6.1 Excitation Source

2.6.1.1 Solid State Lasers[27]

In solid state lasers, the active medium is in the form of a single crystal or a glass. The first successful laser, and one that still finds a widespread use, was a three level laser in which a ruby crystal was the active medium. Ruby is primarily Al_2O_3 but contains a small proportion of Cr^{3+} ions distributed among the Al^{3+} lattice sites, which accounts for the red coloration. The Cr^{3+} ions are the active lasing material.

The Nd:YAG laser is one of the most widely used solid state lasers. It consists of Nd^{3+} ion in a host crystal of yttrium aluminum garnet ($Y_3\ Al_{15}\ O_{12}$). This system offers the advantage of being a four-level laser, which makes it much easier to achieve population inversion than the case of the ruby laser. A neodynium laser operates at a number of wavelengths in the infrared, the band at 1064 nm being most common. The radiant power output at 1064 nm is very high and thus is good enough for frequency doubling which could be used for pumping tunable dye lasers. Figure 2.2 shows the transitions involved in the Nd^{3+} lasers.

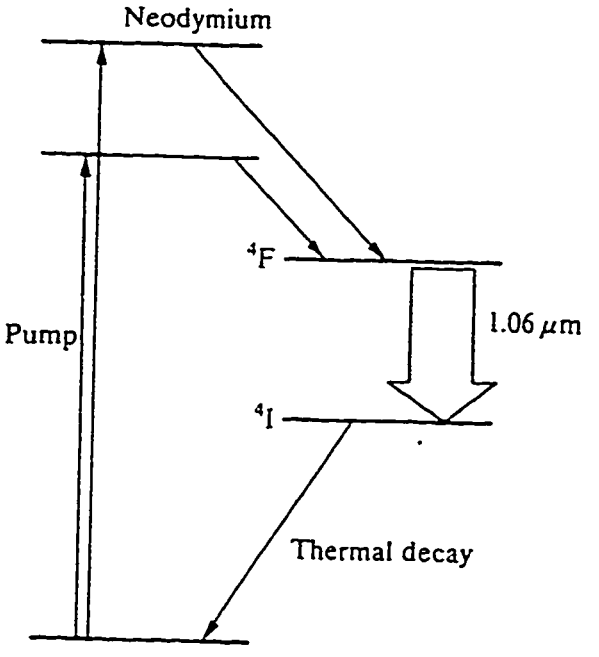

Figure 2.2: The transitions involved in the neodymium laser. The laser action takes place between two excited states, and the population inversion is easier to achieve (adapted from Ref. 27).

2.6.1.2 Dye Lasers[28]

A solid state laser operates at discrete frequencies, and although the frequency required may be selected by suitable optics, the laser cannot be tuned continuously. The active materials in dye lasers are solutions of organic compounds capable of fluorescing in the ultraviolet, visible, or infrared regions. Dye lasers are four-level systems. In contrast to solid state lasers, the lower energy level for laser action is not a single energy but a band of energies arising from the superposition of a large number of closely spaced vibrational and rotational energy states upon the base electronic energy state. Hence, it is possible to scan the wavelength continuously. A commonly used dye is Rhodamine 6G in ethylene glycol (Figure 2.3).

2.6.1.3 Frequency Doubling With Nonlinear Optical Effect[30]

When an electromagnetic wave is transmitted through a deilectric medium, the electromagnetic field of the radiation causes momentary distortion, or polarization, of the valence electrons of the molecules making up the medium. For ordinary radiation the extent of polarization P is directly proportional to the magnitude of the electric field E of the radiation or

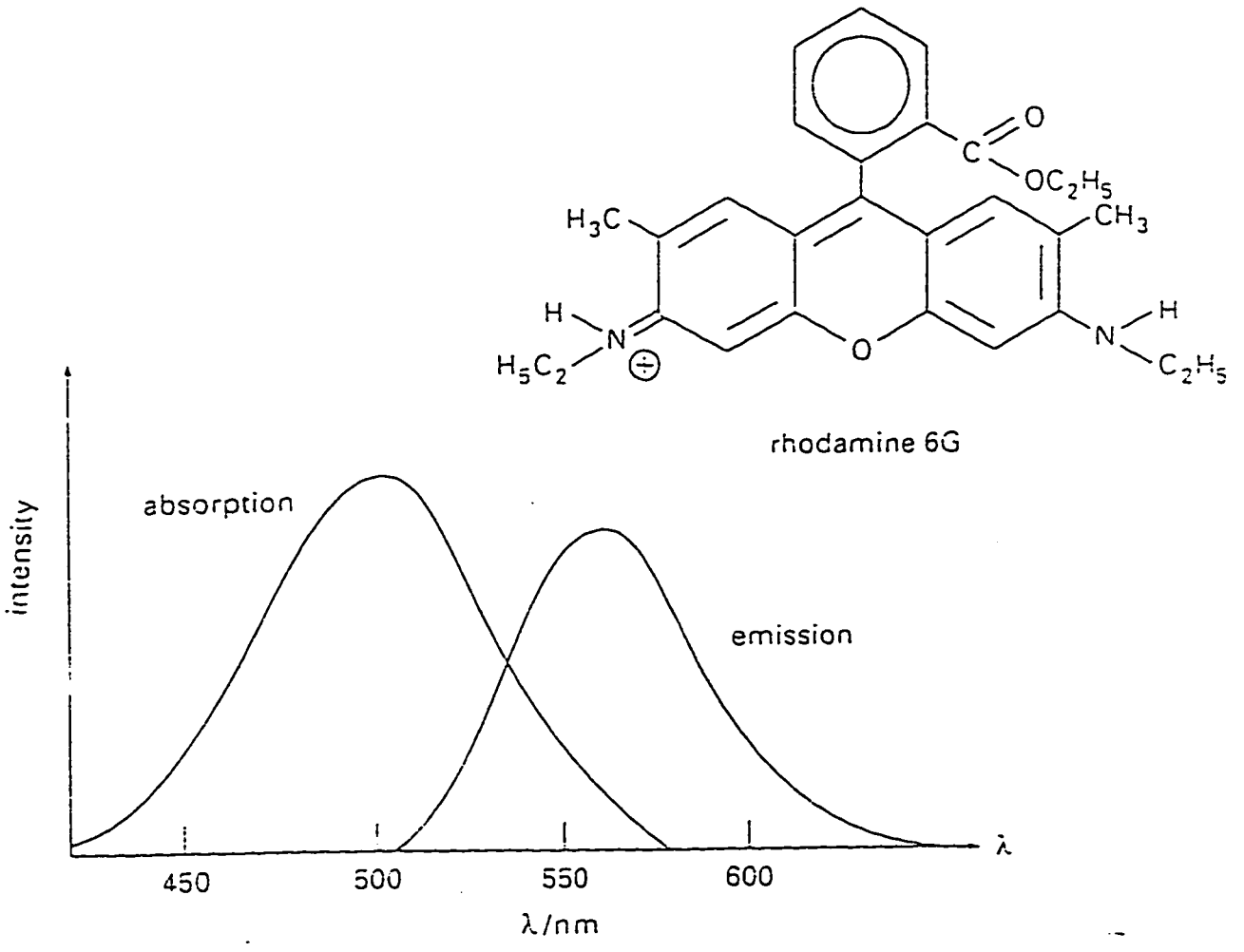

Figure 2.3: The absorption and emission spectra of rhodamine 6G (adapted from Ref. 46).

$$P = \alpha E \qquad (2.1)$$

where α is the proportionality constant. Optical phenomena when this situation prevails are said to be linear.

At high radiation intensities encountered with laser radiation, this relationship breaks down, particularly when E approaches the binding energy of the electrons. Under these circumstances, nonlinear optical effects are observed wherein the relationship between polarization and electrical field is given by the equation

$$P = \alpha E + \beta E^2 + \gamma E^3 + \ldots\ldots \qquad (2.2)$$

where the magnitude of the three constants is in the or of $\alpha > \beta > \gamma$. With high-intensity lasers the second term and sometimes even the third are required to describe the degree of polarization. When only two terms are required, equation (2.2) can be rewritten in terms of angular frequency ω and the maximum of the field strength E_m, therefore

$$P = \alpha E_m \sin \omega t + \beta E_m^2 + \sin^2 \omega t \qquad (2.3)$$

Substituting the trigonometric identity $\sin^2 \omega t = \frac{1}{2}(1-\cos 2\omega t)$ gives

$$P = \alpha E_m \sin \omega t + \frac{\beta E_m^2}{2} (1-\cos 2\omega t) \qquad (2.4)$$

The first term in equation (2.4) is the normal linear term that predominates at low radiation intensities. At sufficiently high intensity, the second order term becomes significant and results in radiation that has a frequency (2ω) that is double that of the incident radiation. This frequency doubling process is now widely used to produce laser frequencies of shorter wavelength. For example, the 1064 nm near-infrared radiation from a Nd:YAG laser can be frequency doubled to produce a 30% yield of green radiation at 532 nm by passing the radiation through a crystalline material such as potassium dihydrogen phosphate.

2.6.2 Mode Locking Technique[27,31,32]

A laser cavity is essentially a region between two mirrors, which reflects the light back and forth. The only wavelength that can be sustained by the cavity satisfy

$$L = N \cdot \frac{\lambda}{2} \qquad (2.6)$$

where N is an integer and L is the length of the cavity. Moreover, not all wavelengths that can be sustained by the cavity are amplified

by the laser medium because many fall outside the frequency range of the laser transitions. The frequencies are separated by value $\Delta\upsilon$ given by

$$\Delta\upsilon = C/2L \qquad (2.7)$$

The relative phases and amplitudes of the longitudinal modes are in general uncorrelated, so that interference effects result in a randomly fluctuating laser output. Mode locking consists of introducing into the optical cavity a device that will cause the phases of the longitudinal modes to be correlated, so that constructive interference effects reinforce the pulse amplitude at a single point, and destructive interference effects result in the cancellation of the amplitude at all other points. The result is a pulse of light, corresponding to the point of maximum constructive interference, oscillating between the end mirrors. The output of the laser is thus a train of pulses that are separated by the time taken for a complete round-trip between the end mirrors; that is

$$\tau = 2L/C \qquad (2.8)$$

which for a typical laser is approximately 12 nanoseconds. It is readily understood according to the Fourier theorem that the greater the number of interfering modes, the greater will be the destructive interference at points other than that at which the phases are

matched, and thus the shorter the temporal width of the oscillating pulse Δt as indicated in equation (2.9). Thus, the pulse width is largest for lasers in which the emission bandwidth of the medium is smallest. And pulse width is given by

$$\Delta t = 4\pi L/(2N + 1)C \qquad (2.9)$$

where N is the number of modes. L is the length of the cavity and C is the speed of light.

2.6.2.1 Passive Mode Locking

Mode locking in both CW and pulsed lasers can be accomplished by either active or passive methods and in some lasers both are used in combination. In each a device is introduced into the laser cavity that modulates the loss or gain of the laser. Passive mode locking is achieved by using a medium in the cavity, usually a dye solution, that has transmission at the laser frequency that is nonlinear with light intensity. As the non-mode-locked light, with its characteristic randomly fluctuating amplitude oscillates in the optical cavity and pass through the saturable absorber, the low-amplitude fluctuations are reduced in intensity to a greater extent than those with large amplitude. The large-amplitude fluctuations regain intensity when they pass through the laser medium, but with low

amplitude experience overall loss. With successive round-trips in the cavity, the process of high-amplitude fluctuations gaining at the expense of low-amplitude fluctuations continues until all of the energy is concentrated in a single pulse in which all of the longitudinal modes are necessarily in phase, and mode locking is the result.

2.6.2.2 Active Mode Locking

Active mode locking is usually performed by placing an acoustoopic device, often a quartz prism, in the laser cavity. A radio frequency (rf) signal is applied, which causes an acoustic wave to be established in the prism and, hence, a periodic change to occur in the prism retractive index. Loss is thus introduced in the cavity due to the diffraction of the beam that occurs in the prism. The diffraction is modulated at twice the frequency of the signal ω applied to the prism and the result is a mode-locked pulse train in which the interpulse spacing is given by the reciprocal of 2ω. This type of active mode locking is often used in continuous-gas and solid-state lasers.

2.6.3 Synchronous Pumping of Dye Lasers[33]

Synchronous pumping is a form of active mode locking that is usually used with organic dye lasers. In this case, a dye laser, whose gain medium consists of a flowing viscous dye solution in a jet, is pumped by a CW mode-locked laser such as an argon ion or Nd:YAG. The pulse nature of the pump source effectively modulates the gain in the dye laser. If the cavity length in the dye laser is exactly adjusted so that the round-trip time is equal to the time between the pulses of the pump laser, then the dye pulse is exactly timed to be amplified by the pump pulse. Considerable shortening of the dye laser pulse is possible in this configuration as illustrated in Figure 2.4. The dye pulse is timed to arrive exactly when the pump laser has raised the gain in the dye medium above the threshold for lasing. The incoming dye pulse is thus rapidly amplified, and in doing so extracts enough gain from the medium to prevent the gain from again achieving the lasing threshold. This action is the result of the large stimulated cross-section of dye molecules relative to the Nd:YAG laser. The cross-sections of dye molecules are about 10^{-16} cm^2, or 1000 times larger. A dye laser pulse passing through the dye would immediately deexcite the dye molecules by stimulated emission. Therefore, the dye laser turns itself off very quickly by stimulated emission, resulting in dye laser pulses much shorter than the pumping pulse duration or the one nanosecond dye molecule decay time.

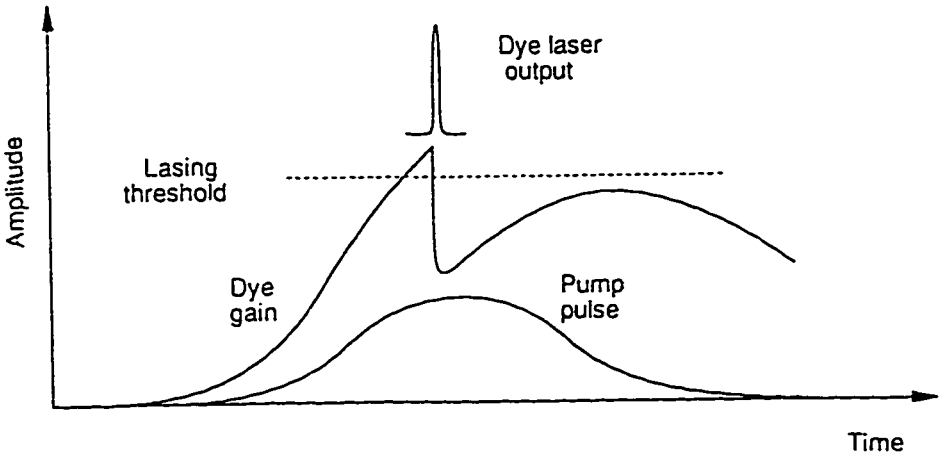

Figure 2.4: Illustration of the mechanism of pulse shortening in synchronously pumped dye lasers.

2.6.4 Cavity Dumping of Synchronously Pumped Dye Lasers[33]

Synchronously pumped dye lasers can be modified to generate more energy per pulse and to achieve wider inter-pulse separation. The partially transmissible output coupler on the extended leg of the dye laser cavity is replaced by a cavity dumper which consists of an acoustooptic deflector centered at the focus of a high reflection astigmatically compensated folded cavity. Each time the cavity dumper is switched on the internally circulating energy is deflected out of the cavity. Since the energy normally coupled out of the synchronously pumped dye laser is only a small fraction of the total intracavity power, higher energy per pulse can be obtained by accessing the power directly with cavity dumping. The desired inter-pulse separation may also be selected by choosing the appropriate dumping rate. For two reasons it is desirable to reduce the laser repetition rate. First, there is an upper limit for the conversion rate of the time to amplitude converter (TAC). Secondly, a high laser repetition rate introduces the problem of incomplete sample recovery between pulses in systems where long-lived transients may be formed.

2.6.5 The Convolution Problem[34]

If the pulse that excites the sample were infinitely narrow, and if the response of the detection were infinitely fast, the observed decay curve would represent the true decay, or δ-pulse, of the sample, G(t). The form of the observed decay, I(t), when the excitation function, E(t), is not a δ-function can be deduced from the theory of impulse functions and leads to what is known by the convolution problem. Convolution, or folding together, occurs because molecules excited by photons at early times are decaying while others are being excited by photons in the tail of the excitation pulse. A simple deduction of the convolution integral is based on the diagram in Figure 2.5. The pump pulse is assumed to be a sum of δ-pulses of amplitude E(t) at any time t. Since the number of sample molecules excited at time t' is proportional to E(t') the number at any later time x - t' is proportional to E(t') G(x - t'). The total number of excited state molecules at time x is then a sum over all times t' preceding time x or, for an infinite sum. In other words,

$$I(t) = \int_0^x E(t')\ G(x - t')\ dt' \qquad (2.10)$$

where I(t) is the observed fluorescence decay, E(t') is the instrumental response function and G (x- t') is the true fluorescence decay of the sample.

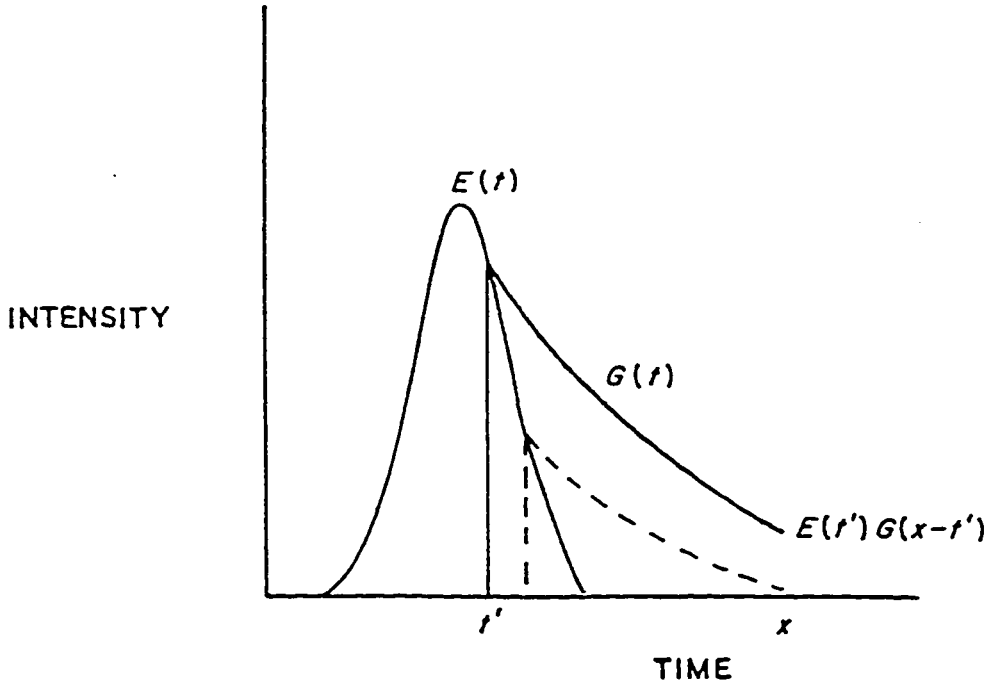

Figure 2.5: Illustration of the effect of convolution. E(t) idealized pump pulse profile; G(t) decay law (assumed single exponential) of sample. (From Ref. 34).

2.6.5.1 Fluorescence Decay Curves Analysis

Deconvolution of fluorescence decay curves has been discussed in detail elsewhere[36,37]. Both these two references recommended least-squares iterative reconvolution and this method was adopted for the present work. With this technique the data points with the highest number of counts are more heavily weighted; moreover any section of the decay curve may be excluded from the analysis. Suppose that the fluorescence decay is a single exponential given by

$$G(t) = a_1 \exp(-t/a_2) \qquad (2.11)$$

and in order to linearize the fitting function, this equation is expanded to first order in a Taylor's expansion as a function of the parameters a_1 and a_2. A linear least-squares search is then carried out to find values of the parameters increments δ_{a1} and δ_{a2} that minimize the reduced χ^2 given by

$$\chi^2 = \sum_{i=n_1}^{n_2} \frac{w_i [Y(ti) - I(ti)]^2}{n_2 - n_1 + 1 - P} \qquad (2.12)$$

where w_i, the weighting factor, is the reciprocal of the number of counts $Y(ti)$ in channel i, n_1 and n_2 are the first and the last channels of the section of the decay to be analyzed, and P is the number of fitting parameters (two for a single exponential fit).

CHAPTER III

RESULTS AND DISCUSSION

CHAPTER III

RESULTS AND DISCUSSION

3.1 Absorption Spectra of Thymine

3.1.1 Ultraviolet Spectra of Thymine at Various pH

Figure 3.1 shows the absorption spectra of thymine in aqueous solutions of different pH values at room temperature. The spectrum of thymine in pH 7 shows a featureless band with a maximum of 265 nm. The same maximum value was reported by Shugar and Fox[37]. Since the pka of thymine[38] is 9.9, the species present in the solutions with pH 1 through pH 7 is the neutral form of thymine. At pH 9, however, the absorption of the anionic form starts to increase because of the deporatanation taking place at position 1[38] (Figure 3.1). As the pH of the medium is increased to 11, the anion exhibits strong absorption at 291 nm. It has been shown that deprotonation of thymine results in a tautomeric equilibrium between its pair of monoanions[38-41]. This conclusion was based on comparison studies between ultraviolet and infrared absorption spectra of the monoanions of thymine (T^-) and uracil with their corresponding 1-methyl and 3-methyl derivatives. Figure 3.2 depicts the ultraviolet absorption spectra of 1-methyl and 3-methyluracil at different pH values indicated on the curves. In the case of 1-methyluracil, the

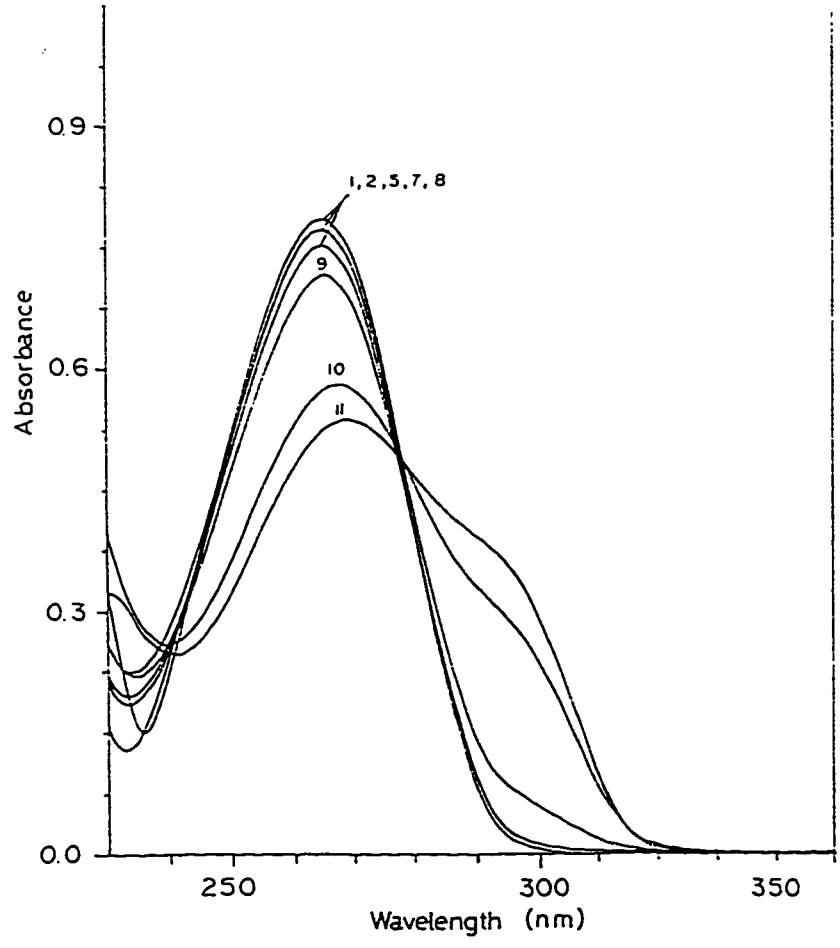

Figure 3.1: Absorption spectra of 10^{-4} M thymine in aqueous solutions of different pH at room temperature (cell path length = 1 cm).

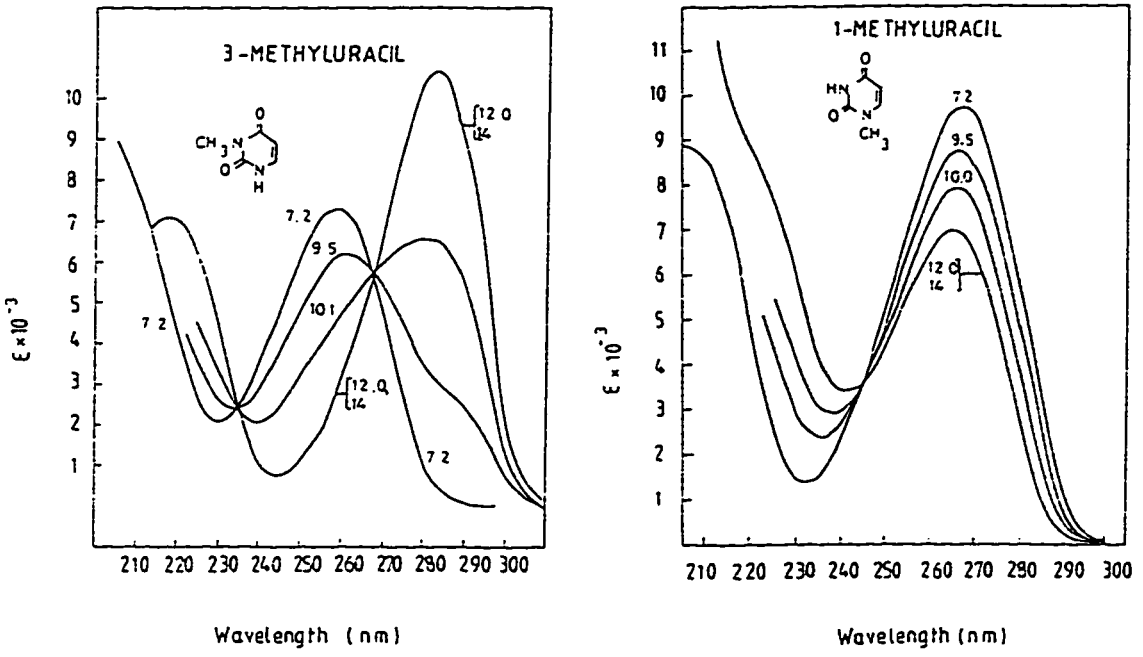

Figure 3.2: Absorption spectra of 3-methyluracil and 1-methyluracil in aqueous solutions of different pH (Adapted from Ref. 39).

peak intensity is lowered as the pH of the medium is increased, but its wavelength is slightly blue shifted. On the other hand, 3-methyl uracil absorbs at longer wavelength. This phenomenon could be explained by the more extended conjugation encountered in the case of the 3-methyluracil anion relative to the 1-methyluracil[40-41]. Using the anions of 1-methyl and 3-methyl derivatives of uracil and thymine as appropriate fixed models of the respective tautomeric monoanions (Figure 3.2) of the parent molecule, it has been demonstrated that the u.v. spectrum of thymine anion, for instance, represents the spectra of the two tautomeric monoanions 1-HT^- (Figure 3.3a) and 3-HT^- (Figure 3.3b)[41], superimposed on each other. A more compelling evidence for the tautomeric nature of thymine monoanion arose from the infrared spectra of thymine monoanion (T^-) And the anions of 1-methylthymine (1-MeT^-) and 3-methylthymine[41] (3-MeT^-). Table 3.1 shows a comparison between 1-MeT^- and 3-MeT^- principal infrared bands and the corresponding bands in the two tautomers of thymine anion[41] (T^-). Apart from the expected differences resulting from the replacement of a proton by a methyl group, the agreement is quite good concluding that the spectrum of T^- represents an equilibrium mixture of the two species 1-HT^- and 3-HT^-. Based on the aforementioned discussion, it was possible to estimate the relative contribution of each tautomer to the absorption spectrum of thymine anion in both u.v. and infrared regions and turned out to be approximately in a 1:1 ratio[41].

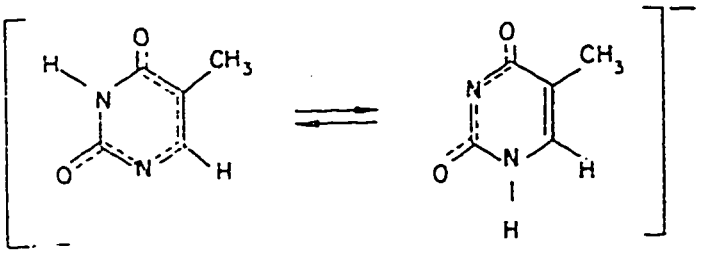

Figure 3.3: Monoanionic tautomers of thymine.

The effect of polarity on the relative contribution of the two monoanionic tautomers supported the previous findings. This was done by recording the u.v. and infrared spectra of thymine and its N-monomethylated derivatives in 0.01 M alkali in dioxane-water, in a volume ratio of[41] 3:1. The enhancement of the assigned bands to 3-HT^- (Table 3.1) and the almost complete disappearance of the bands assigned to 1-HT^- (Table 3.1) were noted. Furthermore, the ultraviolet spectrum of thymine in 75% dioxane- 0.01 M NaOH exhibited a change in the location and shape of the red edge of the absorption band approaching that of 3-MeT^- . Bearing in mind that the dielectric constant of 75% aqueous dioxane is only 16, the apparent increase in the contribution of 3-HT^- was justified as being more aromatic in nature[41] thereby favored in less polar environment (Fig. 3.4).

Although theoretical calculations[44] predict tautomerism in the neutral form of thymine, it is not possible to arrive at such conclusion from the sole consideration of the neutral form absorption spectra. This stems from the low populations of the minor tautomer believed to be 5-methyl-2-hydroxy-4(3H)-pyrimidinone or the keto-enol tautomer (II, Figure 1.1). Therefore, it is very important to resort to fluorescence spectroscopy which is more sensitive to the nature of the ground state as compared to absorption spectroscopy.

Table 3.1*: Frequencies (cm^{-1}) of principal infrared bands in 1-MeT^- (1-methylthymine anion) and 3-MeT^- (3-methylthymine anion) compared with the corresponding bands in the equilibrium mixture of the two tautomeric anions represented by T^-, i.e., 1-HT^- and 3-HT^- in 0.01 N $NaOD/D_2O$.

T^-	1-MeT^-	3-MeT^-
1654	1656	-
1605	-	1615
1581	1593, 1574	
1540	-	1523
1486	1490	-
1470	1458	-
1450	1427	-
1384	1384	-
1357	1361	-

* Adapted from Ref.(41)

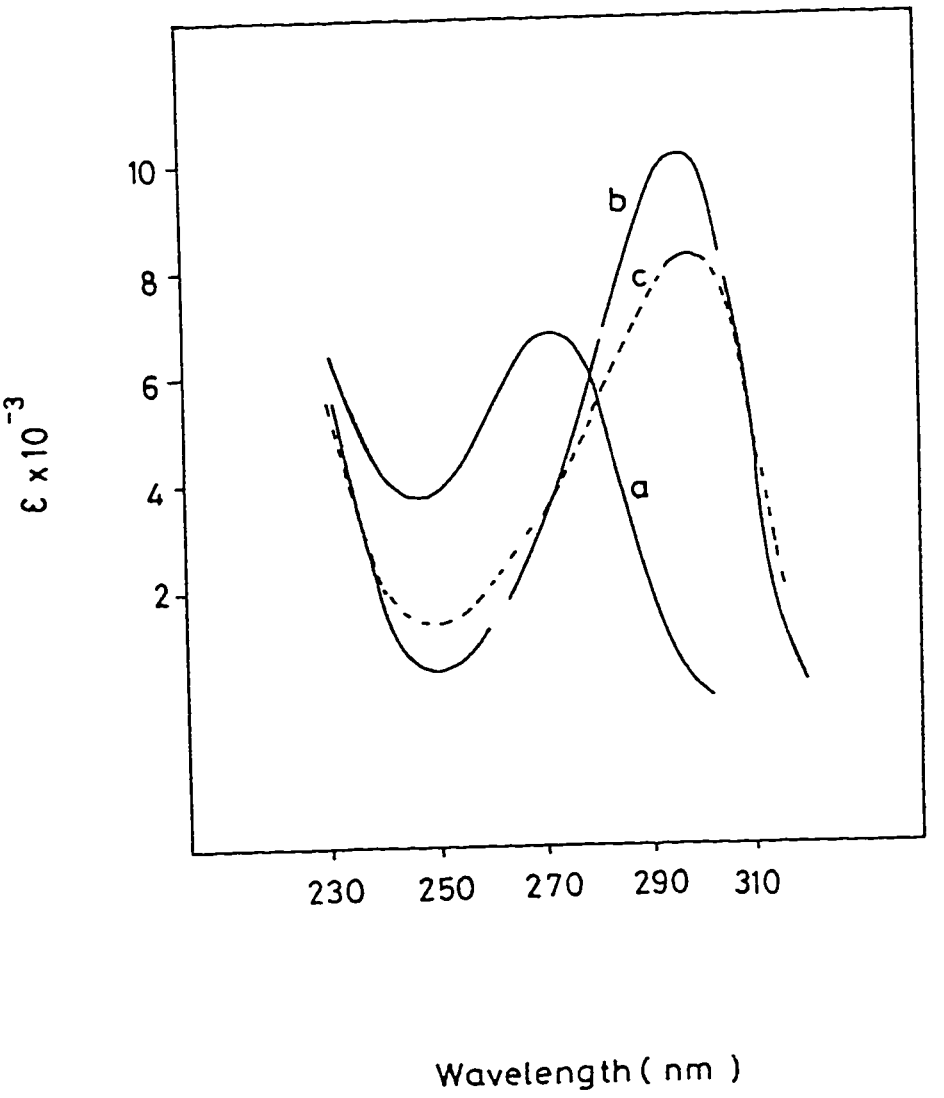

Figure 3.4: Ultraviolet spectra in 0.01 NaOH in 75% dioxane-H_2O: (a) 1-methylthymine, (b) 3-methylthymine and (c) thymine, consisting of a 1:3 mixture of 1-HT^- and 3HT^-. (From Ref. 41).

3.1.2 U.V. Spectra of Thymine at Various Alcohols and Alcohols-Water Mixtures

The absorption spectra of thymine in methanol, ethanol and 1-propanol are shown in Figures 3.5, 3.7 and 3.9. The spectra are almost identical to the spectrum of the neutral form of thymine. This is consistent with the belief that the first absorption band consists of a single intense $\pi\pi^*$ transition in polar-protic solvents[5,7,10]. The absorption band is insensitive to the relative composition in binary mixtures consisting of alcohol and water. The absorption spectra of thymine in 50% binary mixtures of methanol-water, ethanol-water and 1-propanol-water are shown in Figures 3.6, 3.8 and 3.10 respectively.

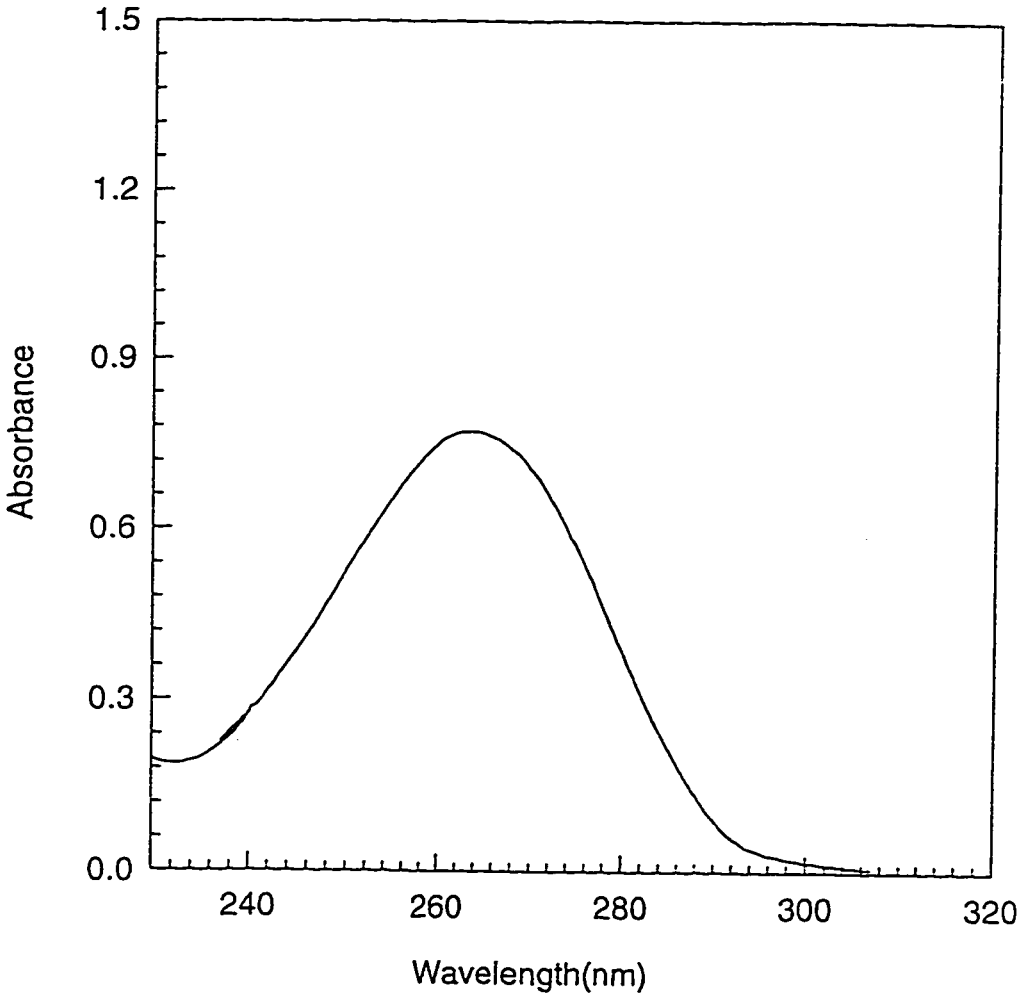

Figure 3.5: Absorption spectrum of 1 x 10^{-4} M thymine in methanol at room temperature.

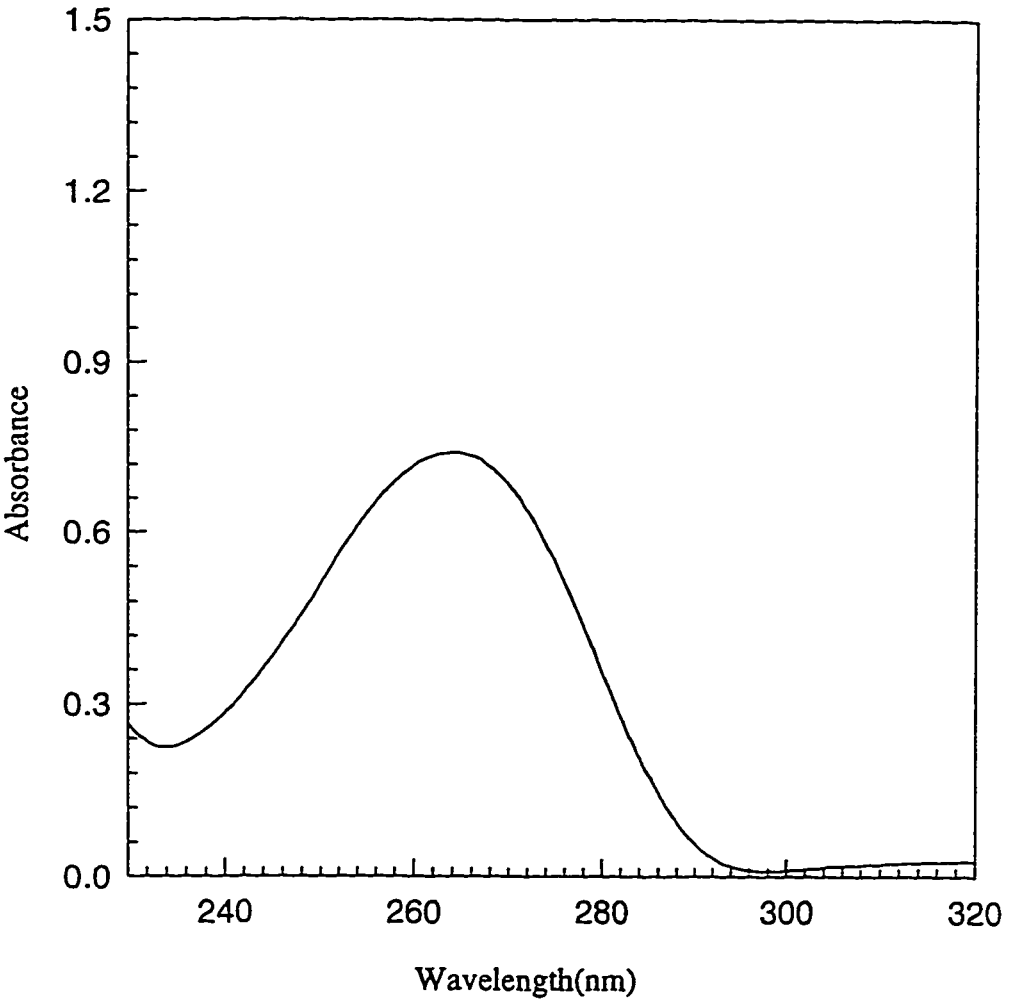

Figure 3.6: Absorption spectrum of 1 x 10^{-4} M thymine in 50% methanol-water mixture at room temperature.

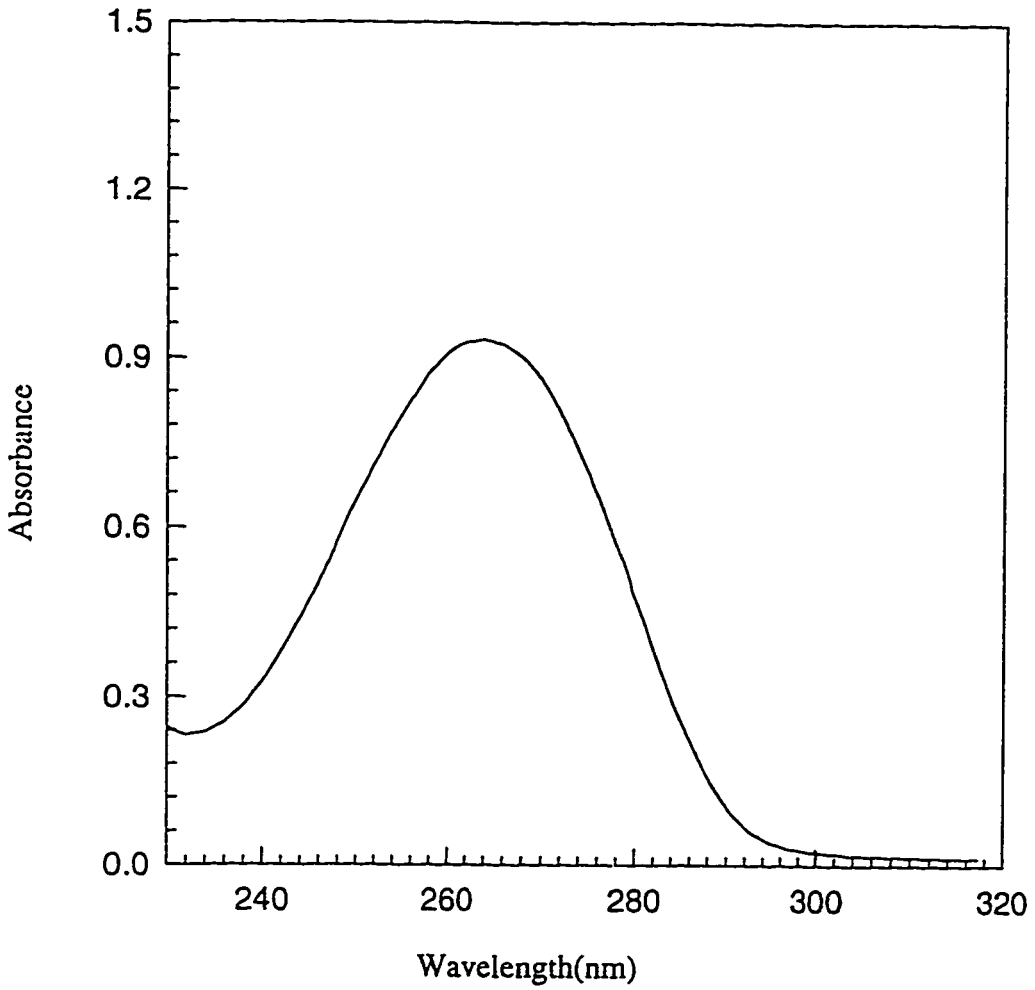

Figure 3.7: Absorption spectrum of 1 x 10^{-4} M thymine in ethanol at room temperature.

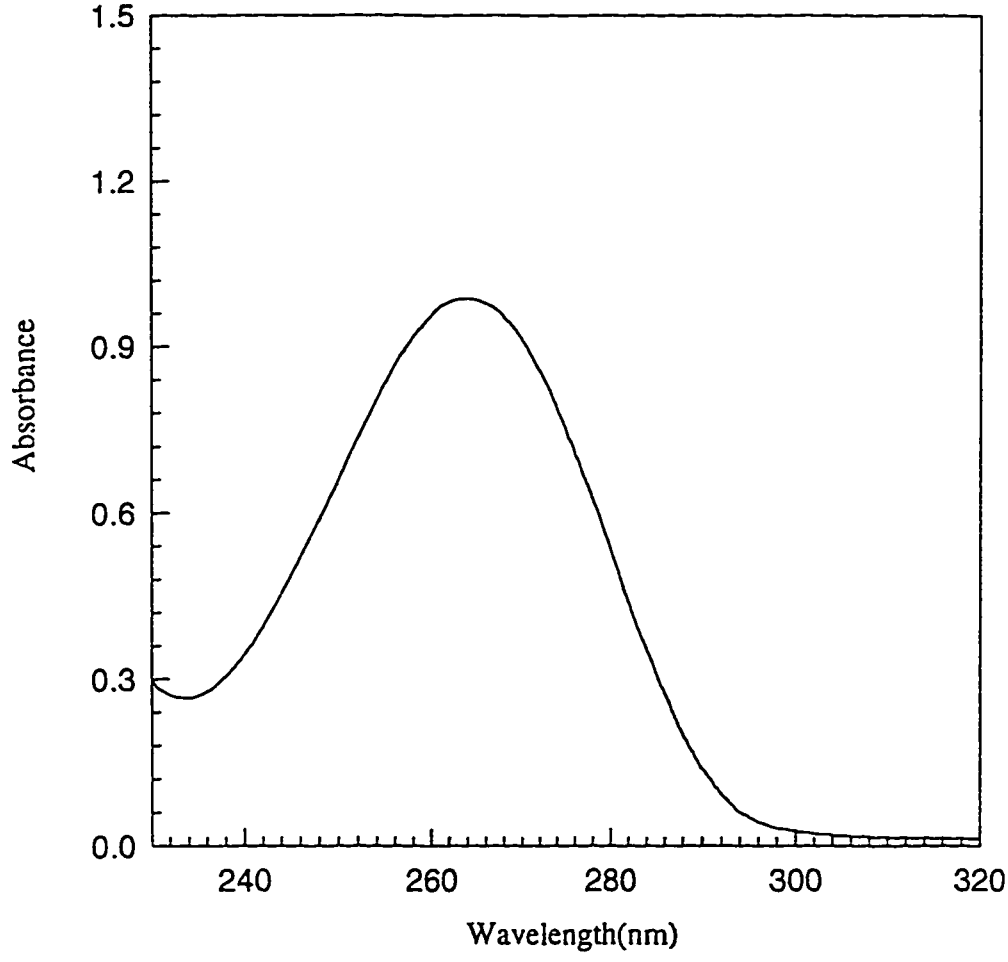

Figure 3.8: Absorption spectrum of 1 x 10^{-4} M thymine in 50% ethanol-water mixture at room temperature.

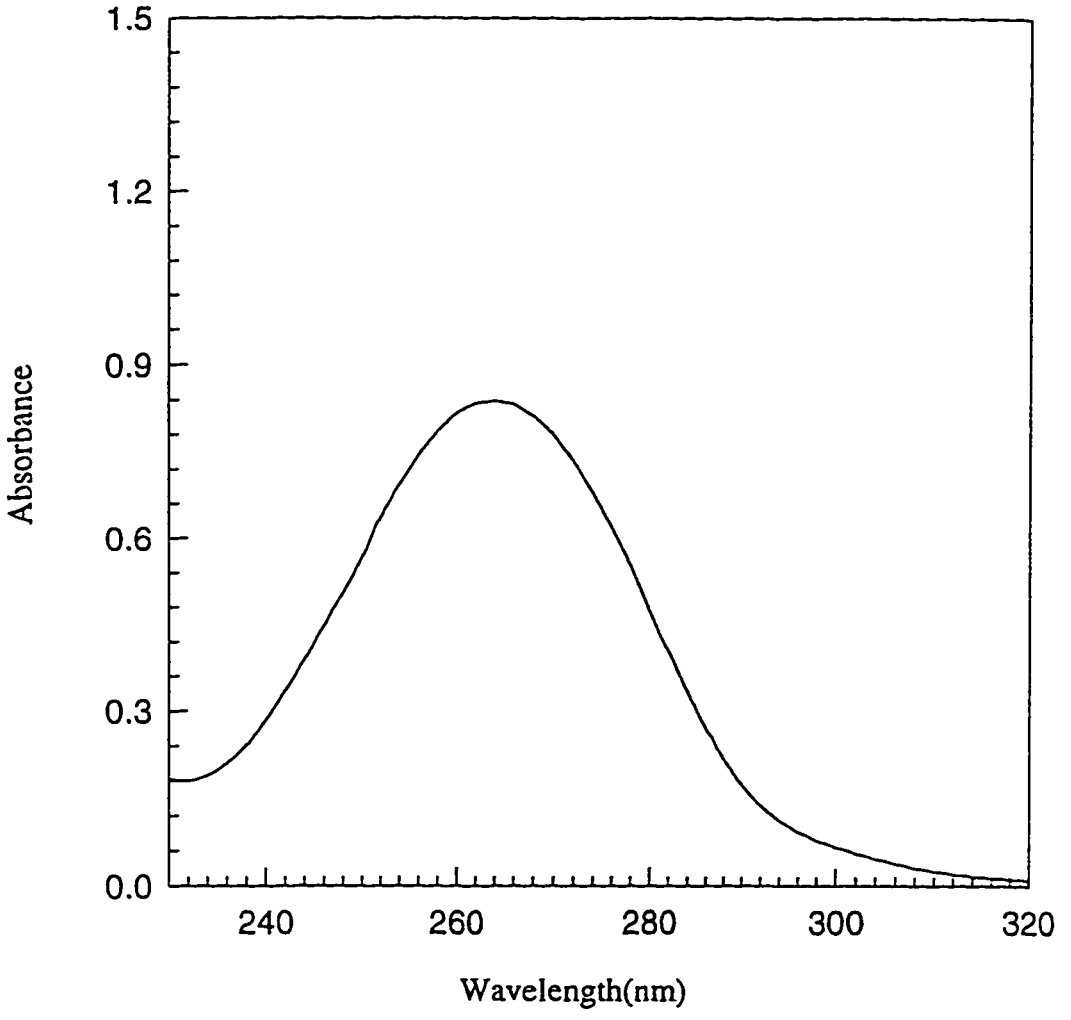

Figure 3.9: Absorption spectrum of 1 x 10^{-4} M thymine in 1-propanol at room temperature.

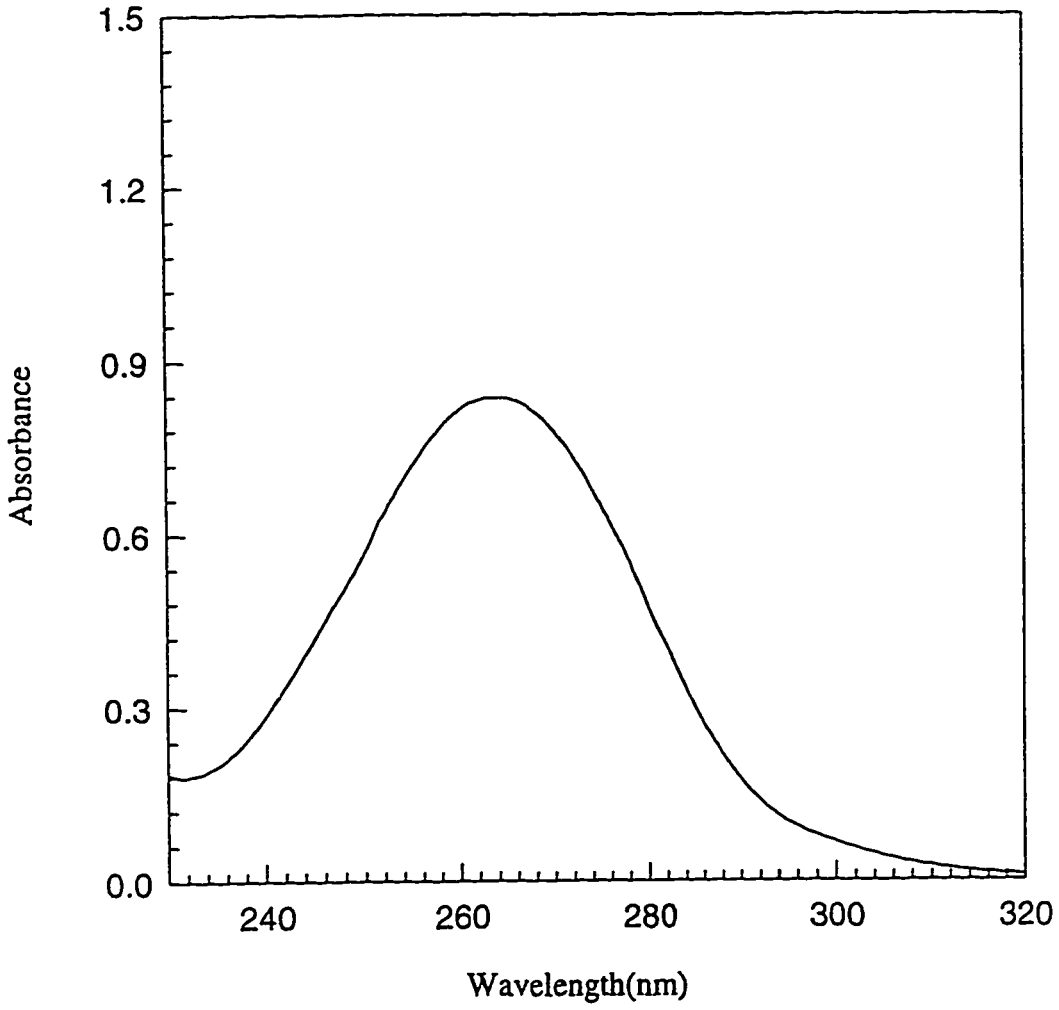

Figure 3.10: Absorption spectrum of 1 x 10^{-4} M thymine in 50% 1-propanol-water mixture at room temperature.

3.2 Steady-state Fluorescence Spectra of Thymine

3.2.1 Fluorescence in Aqueous Solutions of Different pH

Fluorescence spectra of thymine show dependence on the excitation wavelength. Figure 3.11 depicts fluorescence of thymine in an aqueous solution of pH 1. When excited at 260 nm, a broad band with a maximum of 330 nm is observed. When the excitation wavelength is increased to 295 nm, corresponding to the red edge of the absorption band, however, another fluorescence band emerges with a maximum around 390 nm. Moreover, the intensity of the fluorescence increases when the excitation wavelength exceeds 290 nm. The decrease in quantum yield as the excitation wavelength is shortened has been reported by various groups[2-4,43].

Fluorescence spectra of thymine in an aqueous solution of pH 7 at various excitation wavelengths is shown in Figure 3.12. The emission maximum upon excitation at 300 nm is slightly red shifted relative to the corresponding fluorescence spectrum of thymine in pH 1. When excited at 260 nm however, the same emission maximum of pH 1 solution is observed.

The change in the fluorescence shape as the excitation wavelength is varied could be the result of many factors including (1) the presence of two overlapping $n\pi^*$ and $\pi\pi^*$ (2) emission from a minor tautomer and (3) kinetics of competing deactivation processes. The first possibility is ruled out by polarized absorption[21]

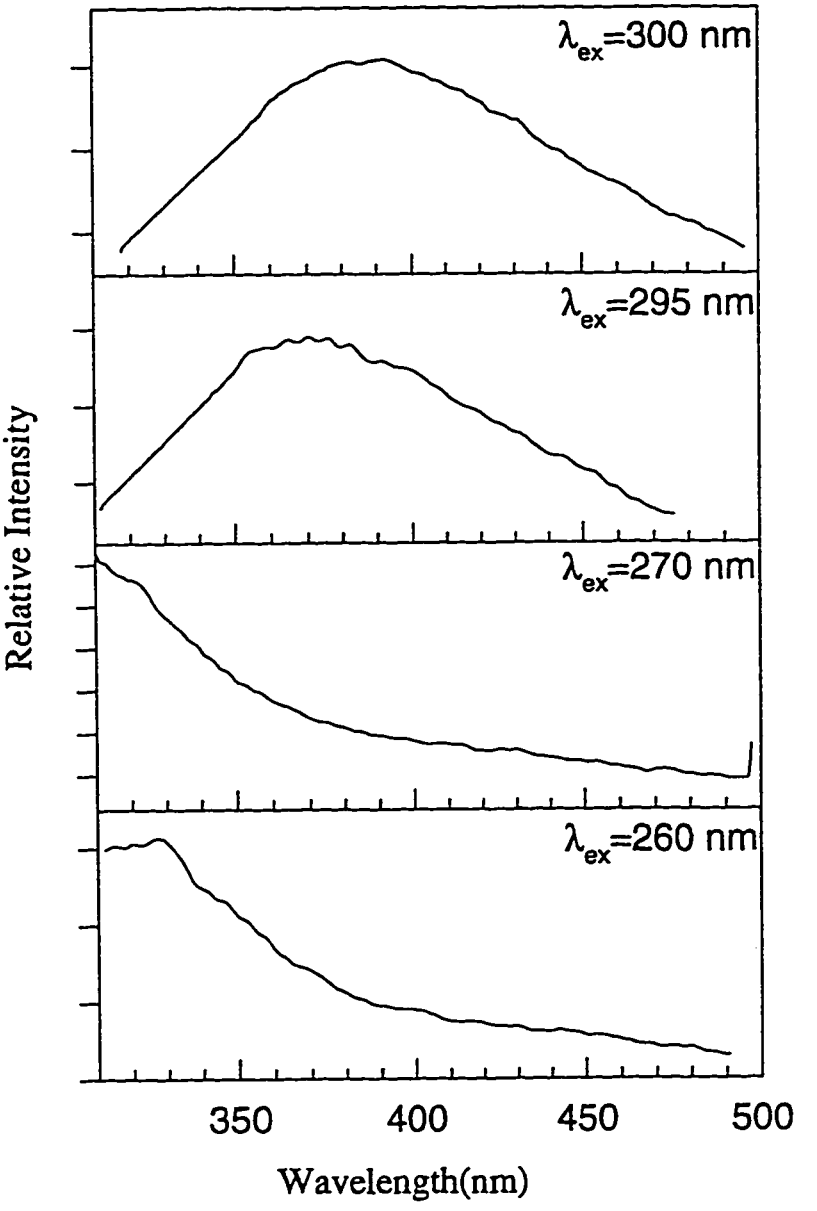

Figure 3.11: Corrected fluorescence spectra of 10^{-4} M thymine in an aqueous solution of pH 1.

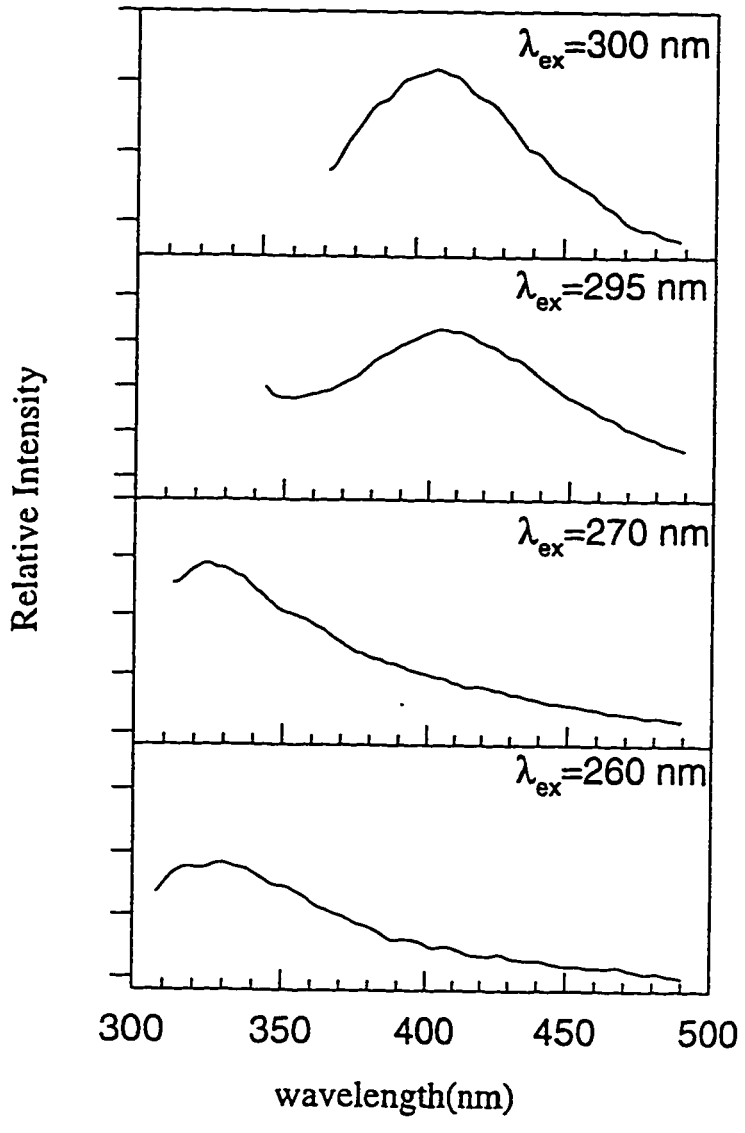

Figure 3.12: Corrected fluorescence spectra of 10^{-4} M thymine in aqueous solution of pH7.

and reflection experiments[22] as well as theoretical calculations which interpret the first absorption band as a single intense $\pi\pi^*$ transition. As far as kinetics of competing deactivation processes are concerned, there is no report of photochemical reaction especially with the low concentration of thymine used in this work. Moreover, there is no evidence for excited state pK_a change[10]. Therefore, one may conclude that the ground state of thymine is heterogeneous comprising of more than one species. Theoretical calculations[44] predict the keto-enol tautomer (II, Fig. 1.1) to be the most stable tautomer next to the dilecto form (I, Fig. 1.1). This is probably the neutral form of 3-HT^- which is one of thymine monoanionic tautomers. It is quite interesting to observed that the excitation wavelength at 295 nm corresponds to the absorption maximum of 3-HT^-, which is one of the monoanionic form of thymine, verified to exist by u.v. and infrared absorption spectra studies on anions of thymine and uracil (see section 3.1.1). Accordingly, the first tautomer, the diketo form, is excited at 260 nm giving a weak maximum at about 330 nm. Whereas the other tautomer, presumably keto-enol, is excited at longer wavelengths (at about 290 nm). The fluorescence of the second tautomer upon excitation at the red edge of the absorption band is compatible with the extended conjugation of the keto-enol tautomer relative to the diketo form and consequently with its higher quantum yield.

Fluorescence spectra in pH 9 and pH 10, shown in Figures 3.13 and 3.14 respectively, exhibit an average behavior of the fluorescence spectra of both the neutral and anionic forms of thymine. This stems from the fact that the pKa of thymine is 9.9 meaning that in pH 9 about 12% of thymine exists as an anionic form[10]. Therefore, in pH 9 and pH 10 solutions, four species contribute to the fluorescence namely; 1-HT$^-$, 3-HT$^-$ and their respective neutral forms.

Figure 3.15 shows the fluorescence spectra of thymine at different excitation wavelength in an aqueous solution of pH 12 where thymine exists almost in the anionic form. The fluorescence of the pH 12 solution is a very broad band with a maximum at around 375 nm. Berens and Wiezchowski[42] have investigated the fluorescence of tautomeric forms of thymine monoanions shown to exist[40,41]. They measured and compared fluorescence and excitation spectra of singly ionized thymine (T$^-$) and of its N-monomethylated derivatives, 3-MeT$^-$ and 1-MeT$^-$. According to their study, the fluorescence spectra of 3-MeT$^-$ and T$^-$ overlap at excitation wavelength of 290 nm at room temperature, whereas they could not detect any fluorescence due to 1-MeT$^-$ at room temperature. It is noteworthy that due to instrument limitation, they were not able to detect any fluorescence with a quantum yield of less than 0.001. At 77 ^oK however, both the N-monomethylated derivatives are fluorescent. Accordingly, the broad band fluorescence observed for

pH 12 solution probably includes overlapping contributions from the two monoanionic tautomeric forms, 1-HT^- and 3-HT^-, with the contribution of the latter being higher.

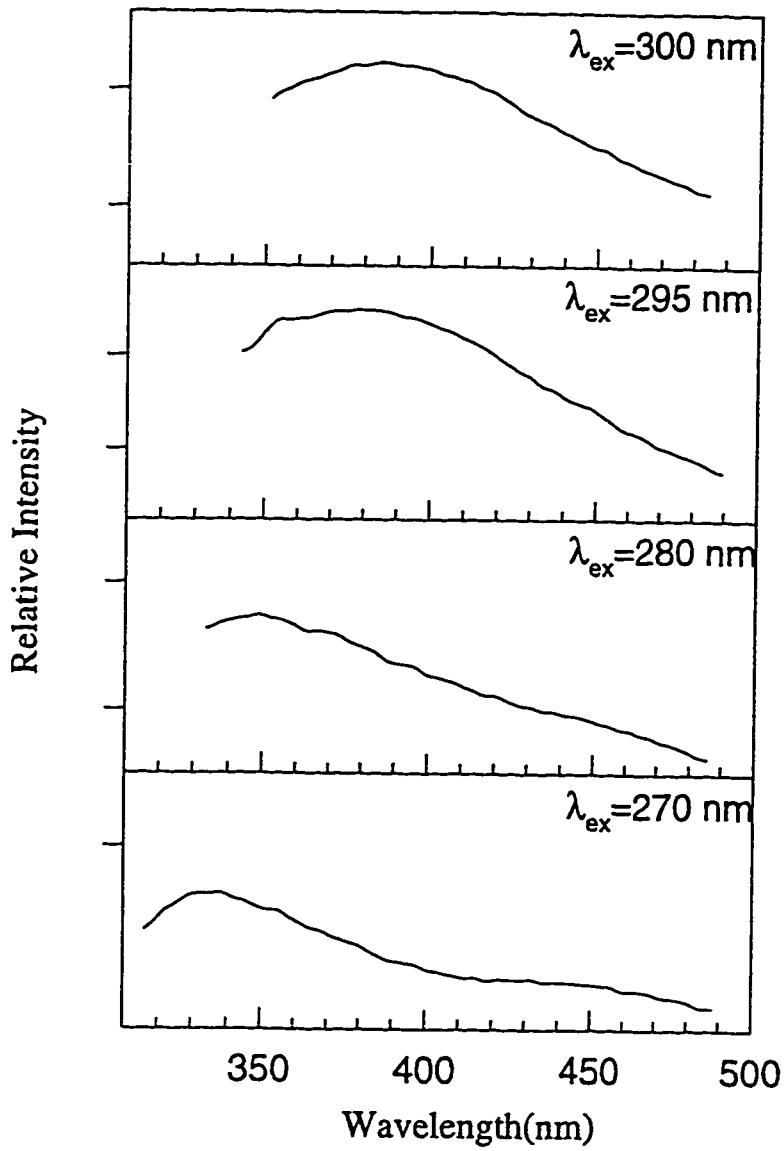

Figure 3.13: Corrected fluorescence spectra of 10^{-4} M thymine in an aqueous solution of pH 9.

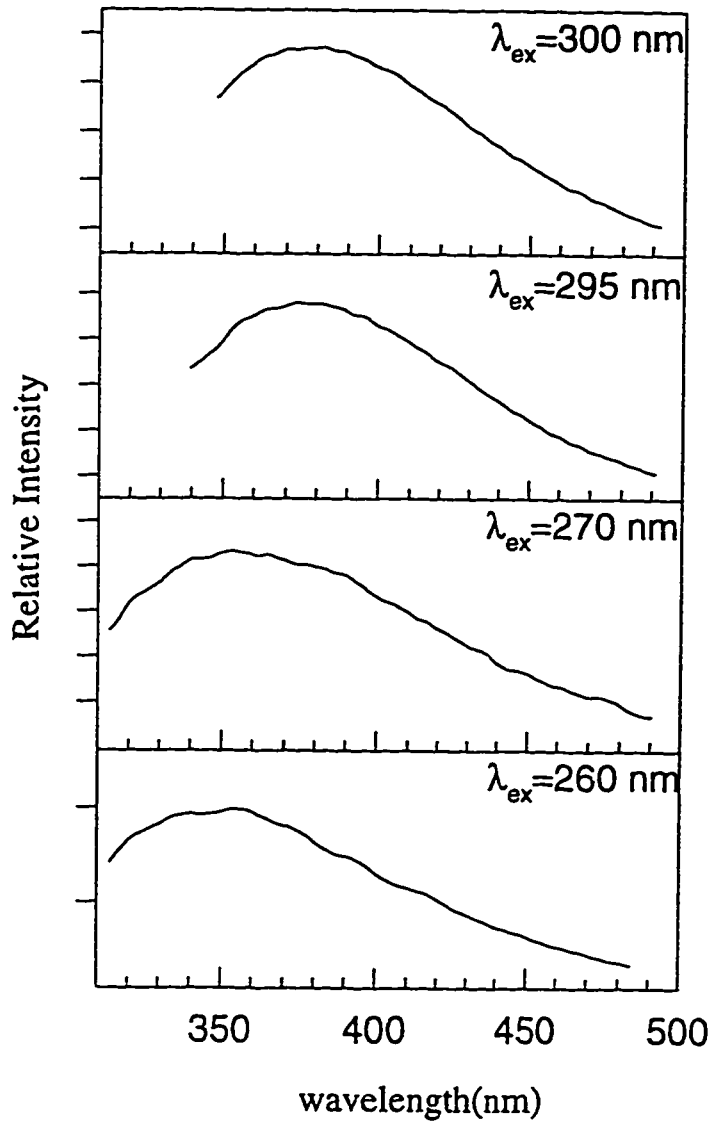

Figure 3.14: Corrected fluorescence spectra of 10^{-4} M thymine in an aqueous solution of pH 10.

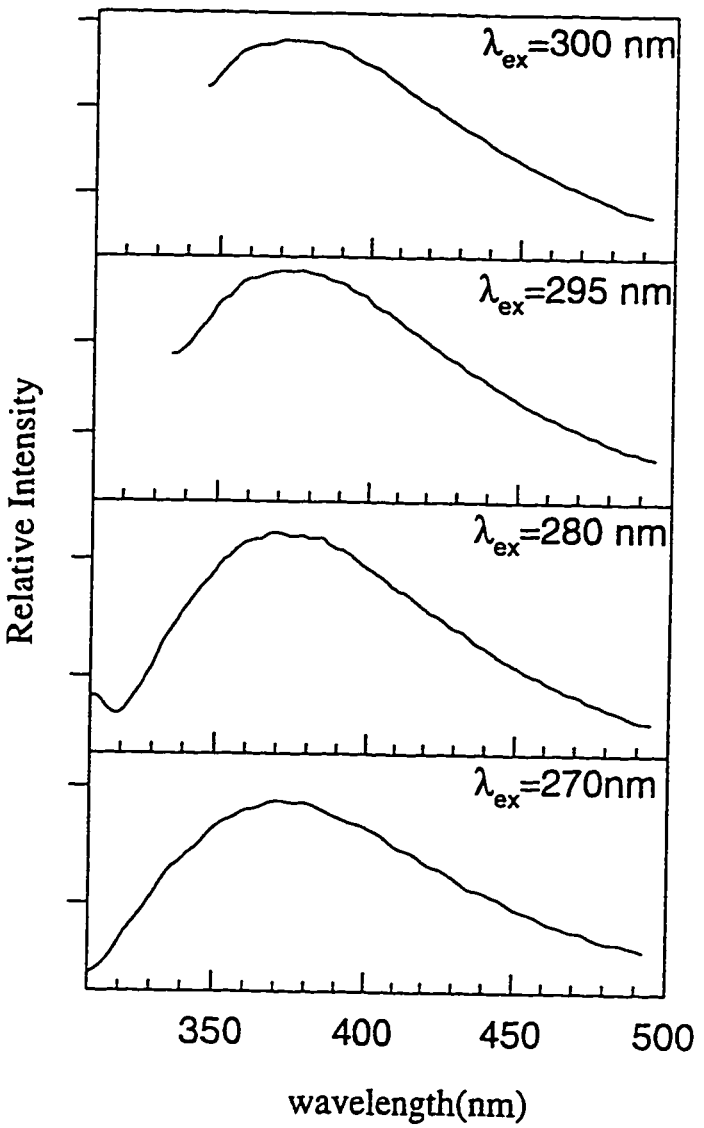

Figure 3.15: Corrected fluorescence spectra of 10^{-4} M thymine in an aqueous solution of pH 12.

3.2.2 Fluorescence Spectra in Various Alcohols and Alcohols-Water Mixtures

Figures 3.16 shows the effect of excitation wavelength on steady-state fluorescence spectra of thymine in 1-propanol. These spectra exhibits structural changes as the excitation wavelength is varied. The observation of these changes stems from the dramatic increase in the quantum yield in 1-propanol and the consequence repression of Raman scattering interference. Upon exciting at 295 nm, a band with a maximum of 360 nm along with two shoulders at 225 nm and 310 nm are observed. As the excitation wavelength is shortened to 280 nm, the previous shoulder at 310 nm emerges into a peak accompanied by a decrease in the intensity of the 325 nm peak and the 360 nm band. Moreover, two shoulders appear at 350 nm and 380 nm.

When excited at 270 nm, further increase in the 310 nm band, a shoulder at 325 nm and a broad band at 355 nm are observed. Further decrease of the excitation wavelength to 260 nm reveals a pronounced increase in the intensity of the peak at 310 nm and disappearance of shoulders at 325 nm and 350 nm. Furthermore, an increase in the intensity of the 380 nm shoulder is observed. Therefore, the bands at 310 nm and 380 nm, showing increase in intensity as the excitation wavelength is shortened, are probably due to one species. Whereas bands at 325 nm, 350 nm and 360 nm, exhibiting high intensity at longer excitation wavelengths are

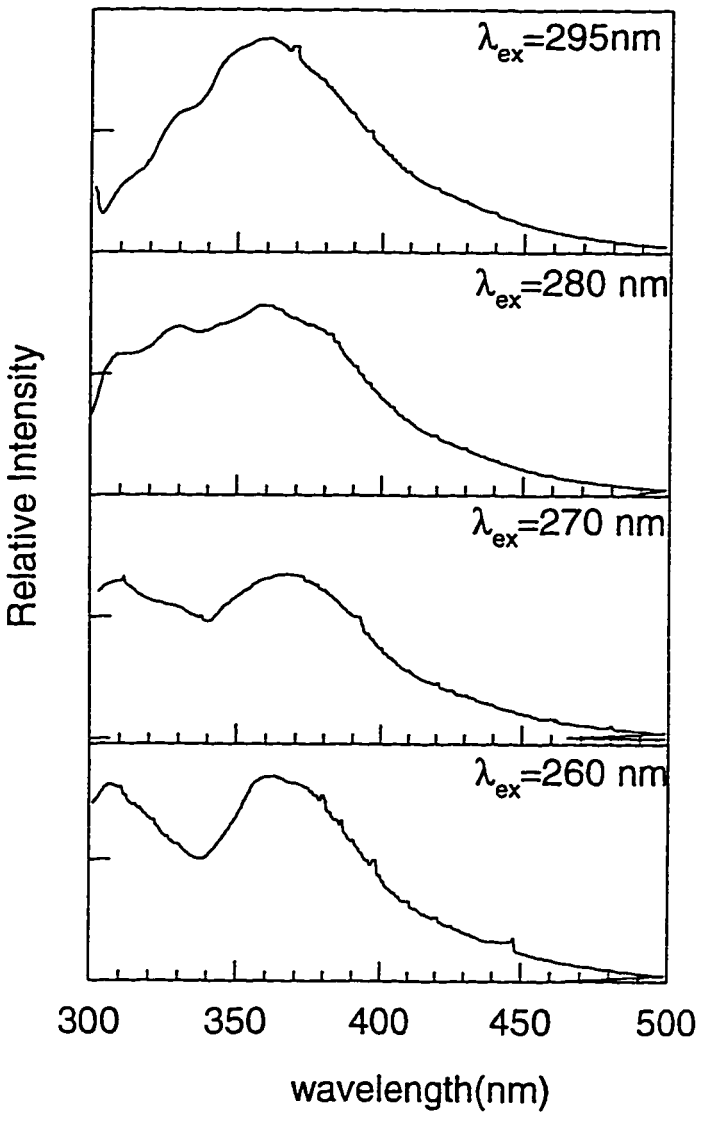

Figure 3.16: Corrected fluorescence spectra of 10^{-4} M thymine in 1-Propanol.

probably to another species. Bearing in mind that the contribution of the diketo tautomer increases as the excitation wavelength is shortened, one may conclude that the bands at 310 nm and 380 nm are due to the diketo tautomer. While the bands at 325 nm, 350 nm and 360 nm are due to the keto-enol tautomer.

Fluorescence spectra of thymine in ethanol and methanol at different excitation wavelengths are shown in Figures 3.17 and 3.18 respectively. Because of the low fluorescence quantum yield in these solvents and the consequent Raman scattering interference, it is difficult to examine the spectra in details. However, the general features of these spectra are in accordance with the fluorescence spectra of thymine in 1-propanol.

The fluorescence spectra of thymine in 50% combination of water and these alcohols does not show any deviation from the corresponding fluorescence spectra of thymine in 1-propanol, ethanol and methanol, as can be seen in Figures 3.19, 3.20 and 3.21, respectively. This is an indication that thymine does not undergo a pK_a shift in the excited state.

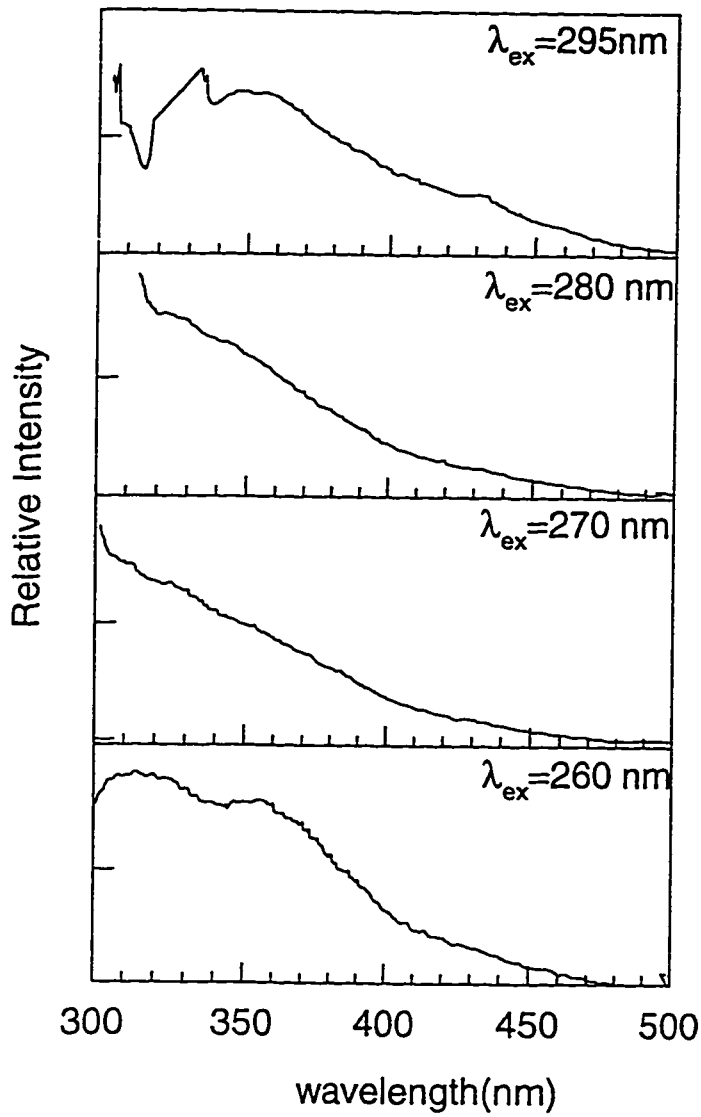

Figure 3.17: Corrected fluorescence spectra of 10^{-4} M thymine in ethanol.

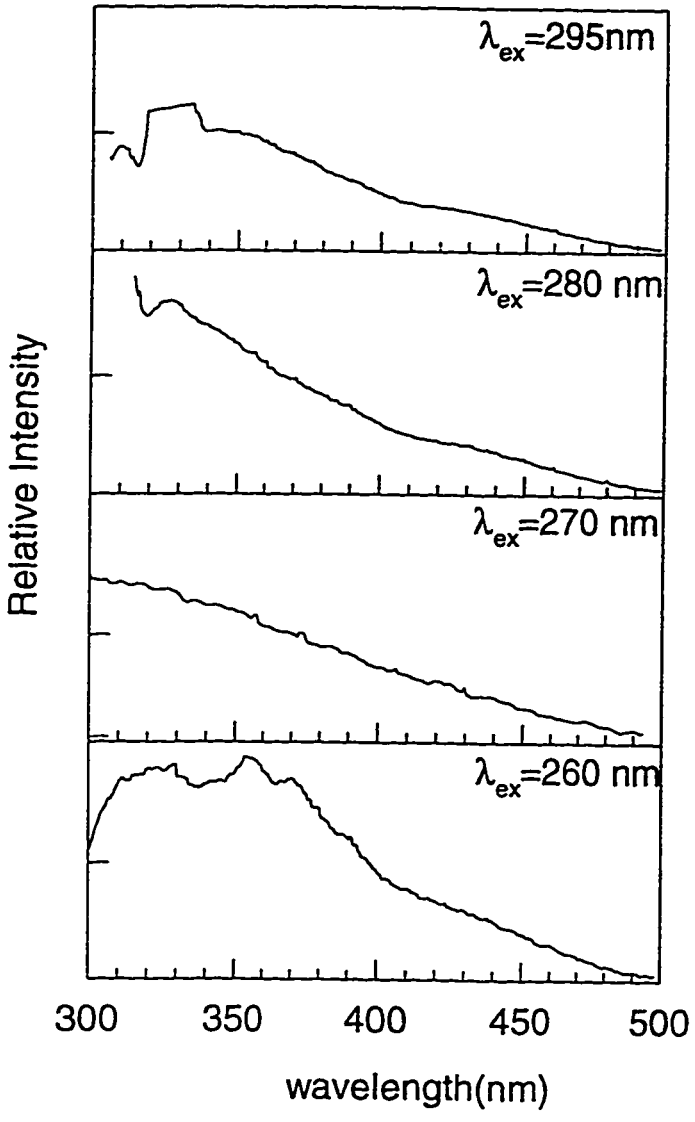

Figure 3.18: Corrected fluorescence spectra of 10^{-4} M thymine in Methanol.

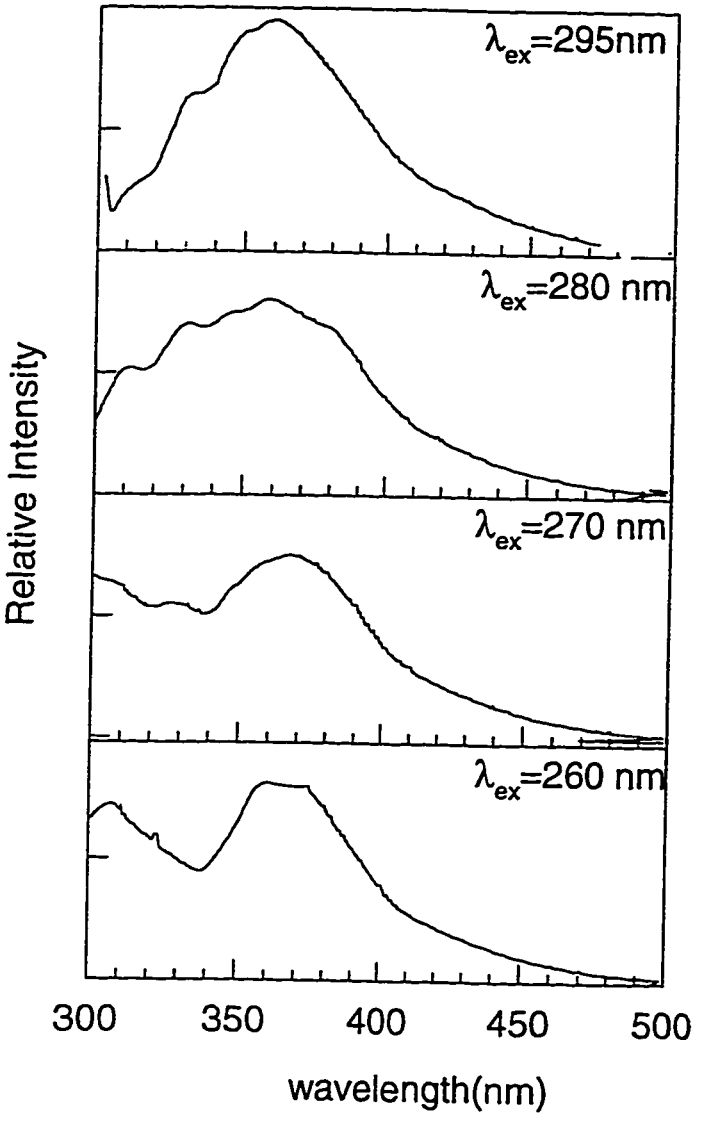

Figure 3.19: Corrected fluorescence spectra of 10^{-4} M thymine 50% 1-Propanol-water mixture.

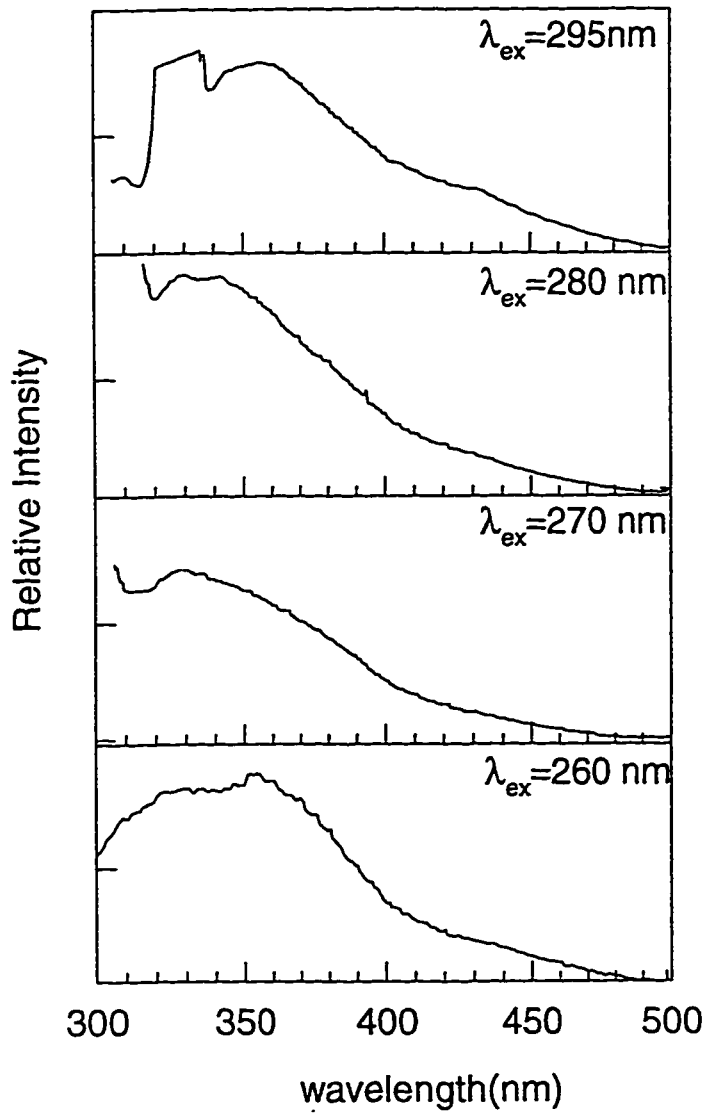

Figure 3.20: Corrected fluorescence spectra of 10^{-4} M thymine in 50% ethanol-water mixture.

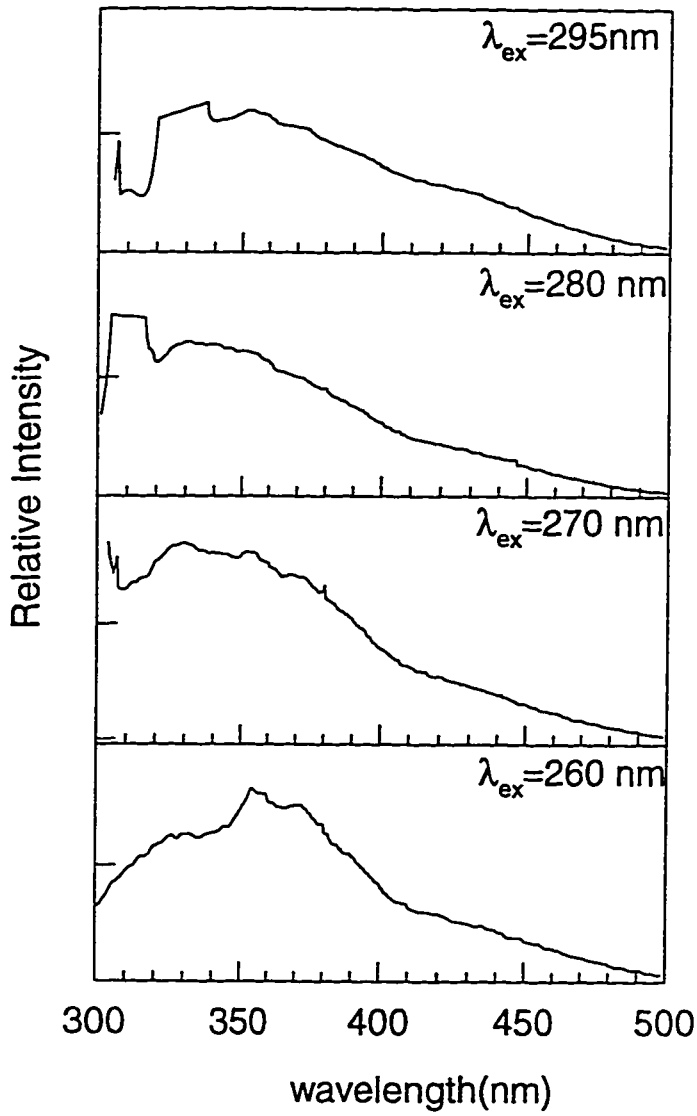

Figure 3.21: Corrected fluorescence spectra of 10^{-4} M thymine in 50% methanol-water mixture.

3.3 Fluorescence Decay of Thymine

3.3.1 Effect of pH on the Fluorescence Decays

The fluorescence decays of thymine in solutions of different pH were collected. Some of these decays are shown in Figure 3.22. The fluorescence decay of thymine in pH 1, 2, 5 and 7 exhibited a biexponential decay with lifetimes of about 0.7 and 4 ns. These values are very close to the lifetimes observed for 5-chlorouracil in an aqueous solution of pH 4[14]. In pH 9 solution, the fluorescence decay of thymine was fitted to a three-exponential with the emergence of new lifetime of less than 100 ps exhibiting high contribution to the fluorescence. This new lifetime arises from the more fluorescent anion, as compared to the neutral form, of thymine. Due to the pulse broadening of 350 ps resulting from the detection system of the single photon counting spectrometer, it was not possible to deconvolute the lifetimes of thymine monoanions tautomers as depicted in Figure 3.22.

The calculated lifetimes (τ_i), normalized preexponential factor ($a_i/\Sigma a_i$), reduced χ^2 values, and the relative quantum yields ($Q = a_i \tau_i/\Sigma a_i \tau_i$) for the different pH solutions are summarized in Table 3.2. A careful examination of the relative quantum yield values reveals that the contribution of the longer life time increases when the emission wavelength is increased from 380 nm to 420 nm. The second observation made here is that, as the pH is increased to 7, the longer life time contribution grows accompanied by an appreciable

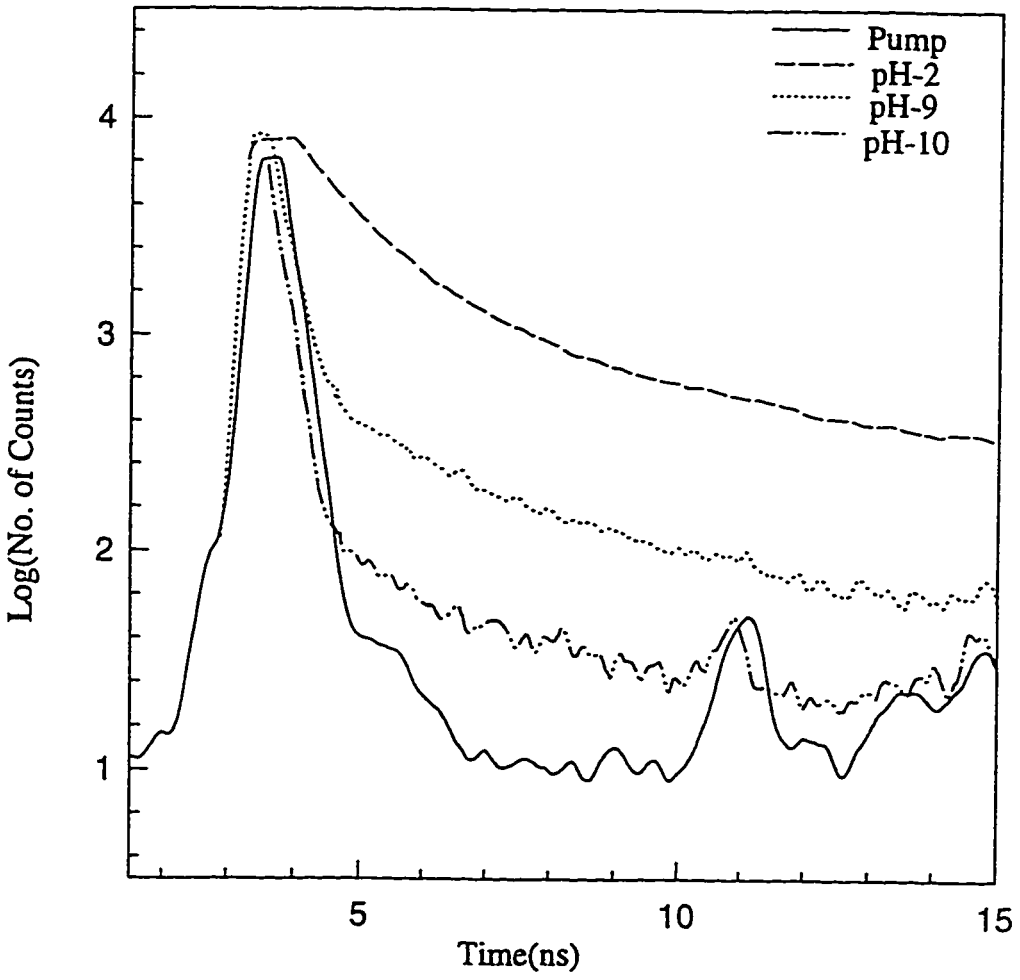

Figure 3.22: Fluorescence decay of 10^{-4} M thymine in different pH aqueous solutions.

Table 3.2: Fuorescence lifetimes (τ_i), normalized preexponential factors (a_i), reduced χ^2 and relative quantum yields ($Q_i = a_i \tau_i / \Sigma a_i \tau_i$) of thymine in aqueous solutions of different pH (λ_{ex} = 295 nm).

Solvent	λ_{em}	τ_1	a_1	Q_1	τ_2	a_2	Q_2	τ_3	a_3	Q_3	χ^2
pH1.0	380	0.615±0.011	0.84	0.43	4.33±0.012	0.16	0.57	-	-	-	1.1
	420	0.704±0.0087	0.74	0.32	4.18±0.0037	0.26	0.68	-	-	-	1.1
pH2.0	380	0.825±0.0019	0.86	0.55	4.07±0.015	0.14	0.45	-	-	-	1.1
	420	0.86±0.063	0.73	0.35	4.47±0.31	0.27	0.65	-	-	-	1.0
pH5.0	380	0.746±0.0073	0.69	0.30	3.91±0.022	0.31	0.70	-	-	-	1.1
	420	0.604±0.062	0.58	0.17	4.16±0.15	0.42	0.83	-	-	-	1.1
pH7.0	380	0.702±0.021	0.65	0.26	3.76±0.045	0.35	0.74	-	-	-	1.1
	420	0.823±0.019	0.41	0.13	3.85±0.017	0.59	0.87	-	-	-	1.0
pH9.0	380	0.602±0.014	0.011	0.058	3.87±0.026	0.009	0.26	0.0774±0.0003	0.98	0.68	0.98
	420	0.693±0.13	0.005	0.050	3.89±0.10	0.005	0.45	0.0330±0.0015	0.99	0.50	1.1

increase in its relative quantum yield for a given emission wavelength. This probably accounts for the red shift of the fluorescence maximum observed for the pH 7 solution relative to the steady-state fluorescence of thymine in pH 1 at excitation wavelength of 295 and 300 nm (Figures 3.11 and 3.12). Therefore, the biexponential decay observed for pH 1, pH 2, pH 5 and pH 7 solutions is ascribed to the heterogeneity in the ground state of thymine. Since the contribution of the shorter lifetime increases at lower emission wavelength, the shorter life time is believed to be due to the neutral diketo tautomer (I, Figure 1.1). The value of the observed shorter lifetime is in accordance with the earlier results of < 0.5 ns for thymine and thymidine in a 1 : 1 mixture of ethanol and methanol[5]. Moreover, it agrees with the value reported for N, N-dimethylthymine incapable of tautomerization measured by Becker and Kogan[5] to be < 0.5 ns in 2-MTHF (2-methyltetrahydrofuran). The longer lifetime is assigned to the fluorescence decay of the keto-enol tautomer (II, Figure 1.1). It was unfortunate to be unable to measure the lifetimes of thymine monoanionic tautomers as the nature of the fluorescence decay profile, if it were biexponential, would have substantiated the argument presented in this work so far. However, the anion fluorescence decay of 5-chlorouracil, a similar fluorophore to thymine the ground state of which is known to consist of two tautomers[14,41], was measured and found to be biexponential[14].

Therefore, with better time resolution detection system, the fluorescence decay of thymine monoanionic tautomers is expected to be biexponential.

3.3.2 Fluorescence Decays of Thymine in Various Alcohol-Water Mixtures

3.3.2.1 Fluorescence Decays in Methanol-Water and Ethanol-Water Mixtures

The fluorescence decays of thymine in methanol-water and ethanol-water mixtures have been found to be biexponential. The calculated lifetimes, normalized preexponential factor values and relative quantum yields for the different methanol-water and ethanol-water mixtures are summarized in Tables 3.3 and 3.4 respectively. As clearly seen, the fluorescence lifetimes are insensitive to the composition of alcohol-water mixtures. This is consistent with the findings of Williams, Renn and Callis[10]. According to their study, thymine does not undergo excited-state pKa change. It is noteworthy that the longer lifetime, the keto-enol tautomer, increases before it levels off in 80% methanol or ethanol solutions. The relative contribution of the two tautomers is also insensitive to the composition of the alcohol-water mixtures. This is probably a result of invarience in the pH of alcohol-water mixtures causing no change in equilibrium of the two tautomers.

Table 3.3: Fuorescence lifetimes (τ_i), normalized preexponential factors (a_i), reduced χ^2 and relative quantum yields ($Q_i = a_i \tau_i / \Sigma a_i \tau_i$) of thymine in methanol-water mixture (% CH_3OH by Volume).

CH_3OH	λ_{em}	τ_1	a_1	Q_1	τ_2	a_2	Q_2	χ^2
100%	380	1.20±0.0033	0.691	0.386	4.26±0.012	0.309	0.614	1.1
	400	1.34±0.0089	0.744	0.482	4.19±0.032	0.256	0.518	1.1
90%	380	1.19±0.14	0.650	0.308	4.96±0.40	0.350	0.692	1.1
	400	1.38±0.025	0.762	0.486	4.68±0.062	0.238	0.514	1.0
80%	380	1.21±0.15	0.678	0.309	5.70±0.052	0.322	0.691	1.0
	400	1.34±0.11	0.763	0.456	5.14±0.071	0.237	0.544	1.0
70%	380	1.41±0.026	0.741	0.409	5.81±0.15	0.259	0.591	1.1
	400	1.39±0.022	0.779	0.491	5.10±0.100	0.221	0.509	1.1
60%	380	1.40±0.024	0.783	0.474	5.61±0.15	0.217	0.526	1.1
	400	1.49±0.0081	0.862	0.638	5.27±0.10	0.138	0.36*	1.1
50%	380	1.74±0.004	0.805	0.496	5.86±0.0038	0.195	0.504	1.0
	400	1.43±0.017	0.890	0.670	5.72±0.17	0.110	0.33*	1.0
40%	380	1.00±0.012	0.532	0.168	5.61±0.026	0.468	0.832	1.0
	400	1.00±0.0063	0.495	0.154	5.37±0.012	0.505	0.84*	1.1
30%	380	1.16±0.013	0.663	0.290	5.60±0.078	0.337	0.710	1.0
	400	1.17±0.003	0.742	0.402	5.01±0.002	0.258	0.598	1.0

Table 3.4: Fuorescence lifetimes (τ_i), normalized preexponential factors (a_i), reduced χ^2 and relative quantum yields ($Q_i = a_i \tau_i / \Sigma a_i \tau_i$) of thymine in ethanol-water mixture (% Ethanol by Volume).

Ethanol	λ_{em}	τ_1	a_1	Q_1	τ_2	a_2	Q_2	χ^2
100%	380	1.61±0.016	0.535	0.292	4.47±0.03	0.465	0.707	1.0
	400	1.23±0.087	0.504	0.215	4.58±0.012	0.496	0.785	1.1
90%	380	1.01±0.091	0.576	0.193	5.72±0.062	0.424	0.807	1.1
	400	1.00±0.10	0.600	0.206	5.81±0.038	0.400	0.794	1.1
80%	380	1.05±0.068	0.566	0.191	5.75±0.18	0.434	0.809	1.1
	400	1.00±0.032	0.550	0.200	5.02±0.060	0.450	0.804	1.1
70%	380	1.37±0.059	0.401	0.139	5.68±0.058	0.599	0.861	1.0
	400	1.26±0.12	0.394	0.141	5.01±0.15	0.606	0.859	1.0
60%	380	1.08±0.22	0.346	0.102	5.00±0.024	0.654	0.897	1.0
	400	1.24±0.054	0.403	0.136	5.30±0.052	0.597	0.864	1.1
50%	380	1.36±0.068	0.348	0.114	5.62±0.067	0.652	0.886	1.1
	400	1.37±0.057	0.402	0.136	5.86±0.050	0.598	0.864	1.1
40%	380	1.17±0.14	0.388	0.110	5.96±0.11	0.612	0.889	1.0
	400	1.14±0.032	0.417	0.124	5.75±0.028	0.583	0.876	1.1
30%	380	1.01±0.20	0.388	0.100	5.78±0.033	0.612	0.900	1.1
	400	1.03±0.0025	0.385	0.103	5.62±0.0036	0.615	0.897	1.1
20%	380	1.00±0.078	0.456	0.129	5.67±0.018	0.544	0.871	1.0
	400	1.02±0.18	0.458	0.132	5.67±0.046	0.542	0.868	1.1

3.3.2.2 Fluorescence Decay of Thymine in 1-Propanol Water Mixtures

Table 3.5 summarizes the lifetimes, normalized preexponential factor values and the relative quantum yields for thymine in 1-propanol-water mixtures. As clearly seen, the lifetimes of the keto-enol tautomer is observed to increase as water concentration increases. This phenomenon is also observed in methanol-water and ethanol-water but to much less extent. As shown in Tables 3.6 and 3.7, many mixtures of organic solvents with water (e.g., alcohols, DMSO) the viscosity goes through maximum as the fraction organic component is increased. As depicted in Figures 3.23 and 3.24, the lifetime of the keto-enol tautomer increases linearly with the viscosity up to the maximum viscosity after which it varies non-linearly towards the value for the pure 1-propanol component. This kind of behavior has been noticed for certain dyes molecules which are capable of forming hydrogen bonding with all the solvents except water[47]. In cresyl violet, for example, there is a strong hydrogen bonding interaction with the amino groups acting as donors. Although water is normally regarded as a strong hydrogen bonding solvent it seems that in the case of these dyes that the water-water interaction is greater than the water-dye interaction. As far as thymine is concerned, it is believed that the model used to explain the similar behavior in those dyes molecules[47] could be applied in this case. The implication is that in the linear region the organic component, 1-propanol in this case, is involved in the water

hydrogen bonding networks rather than solvating the keto-enol tautomer. This extends up to the maximum viscosity. In the non-linear region above the maximum viscosity the structure of the solvent is broken up due to the excess of 1-propanol which is then available to solvate the keto-enol tautomer.

Table 3.5: Fuorescence lifetimes (τ_i), normalized preexponential factors (a_i), reduced χ^2 and relative quantum yields ($Q_i = a_i \tau_i / \Sigma a_i \tau_i$) of thymine in 1-Propanol-water mixture (% 1-Propanol by Volume).

1-Propanol	λ_{em}	τ_1	a_1	Q_1	τ_2	a_2	Q_2	χ^2
100%	380	1.281±0.053	0.575	0.197	6.65±0.11	0.425	0.803	1.2
	400	1.28±0.001	0.583	0.210	6.72±0.0061	0.417	0.790	1.1
90%	380	1.35±0.062	0.589	0.196	7.92±0.032	0.411	0.804	1.1
	400	1.33±0.012	0.629	0.229	7.60±0.079	0.371	0.779	1.1
80%	380	1.33±0.0016	0.583	0.186	8.11±0.0063	0.417	0.814	1.1
	400	1.31±0.0572	0.618	0.208	8.05±0.034	0.382	0.792	1.0
70%	380	1.34±0.068	0.550	0.156	8.86±0.035	0.450	0.844	1.1
	400	1.28±0.014	0.571	0.168	8.45±0.057	0.429	0.832	1.1
60%	380	1.36±0.036	0.581	0.173	9.02±0.15	0.419	0.827	1.1
	400	1.35±0.035	0.575	0.169	8.97±0.16	0.425	0.831	1.1
50%	380	1.33±0.036	0.570	0.162	9.11±0.14	0.430	0.838	1.1
	400	1.32±0.001	0.595	0.176	9.06±0.003	0.405	0.824	1.0
40%	380	1.40±0.055	0.631	0.198	9.71±0.43	0.369	0.802	1.0
	400	1.45±0.004	0.698	0.257	9.70±0.001	0.302	0.743	1.0
30%	380	1.55±0.14	0.513	0.129	11.0±0.74	0.487	0.871	1.1
	400	1.55±0.017	0.516	0.133	10.7±0.76	0.484	0.867	1.1
20%	380	1.25±0.0063	0.548	0.136	9.62±0.024	0.452	0.864	1.1
	400	1.12±0.074	0.528	0.123	8.76±0.27	0.480	0.877	1.1
10%	380	1.13±0.012	0.604	0.170	8.37±0.050	0.396	0.829	1.1
	400	1.19±0.036	0.550	0.153	8.06±0.10	0.450	0.847	1.0
0%	380	0.714±0.004	0.503	0.139	4.50±0.010	0.496	0.861	1.1
	400	0.711±0.012	0.534	0.150	4.73±0.3	0.466	0.850	1.0

Table 3.6: Relative viscosity (η/η_o) and lifetimes of the keto-enol tautomer in 1-propanol-water mixtures at λ_{em} = 380 nm.

Vol. % 1-Propanol	η/η_o*	Lifetime τ (ns)
100	2.223	6.55 ± 0.11
90	2.590	7.92 ± 0.032
80	2.909	8.11 ± 0.0063
70	3.135	8.86 ± 0.035
60	3.197	9.02 ± 0.15
50	3.096	9.11 ± 0.14
40	2.894	9.71 ± 0.43
30	2.427	11.0 ± 0.74
20	2.102	9.62 ± 0.024
10	1.446	8.37 ± 0.050
0	1.000	4.50 ± 0.010

* Taken from Ref.(45)

Table 3.7: Relative viscosity (η/η_o) and lifetimes of the keto-enol tautomer in 1-propanol-water mixtures at λ_{em} = 400 nm.

Vol. % 1-Propanol	η/η_o*	Lifetime τ (ns)
100	2.223	6.72 ± 0.0061
90	2.590	7.60 ± 0.079
80	2.909	8.05 ± 0.034
70	3.135	8.45 ± 0.057
60	3.197	8.97 ± 0.16
50	3.096	9.06 ± 0.003
40	2.894	9.70 ± 0.001
30	2.427	10.70 ± 0.76
20	2.102	8.70 ± 0.27
10	1.446	8.06 ± 0.10
0	1.000	4.73 ± 0.03

* Taken from Ref.(45)

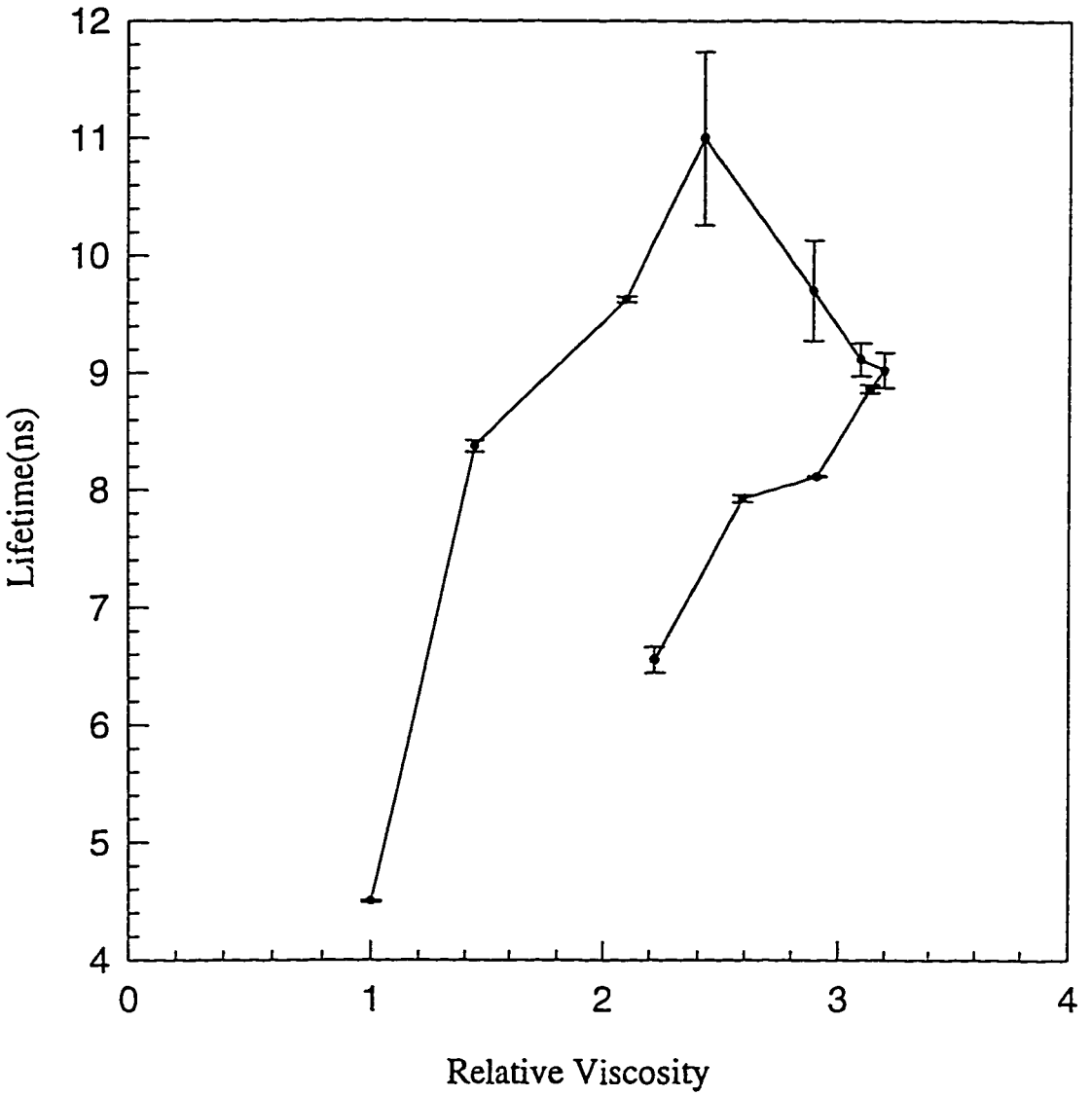

Figure 3.23: Correlation of the keto-enol lifetimes and the relative viscosities of 1-propanol-water mixtures at 380 nm emission wavelength.

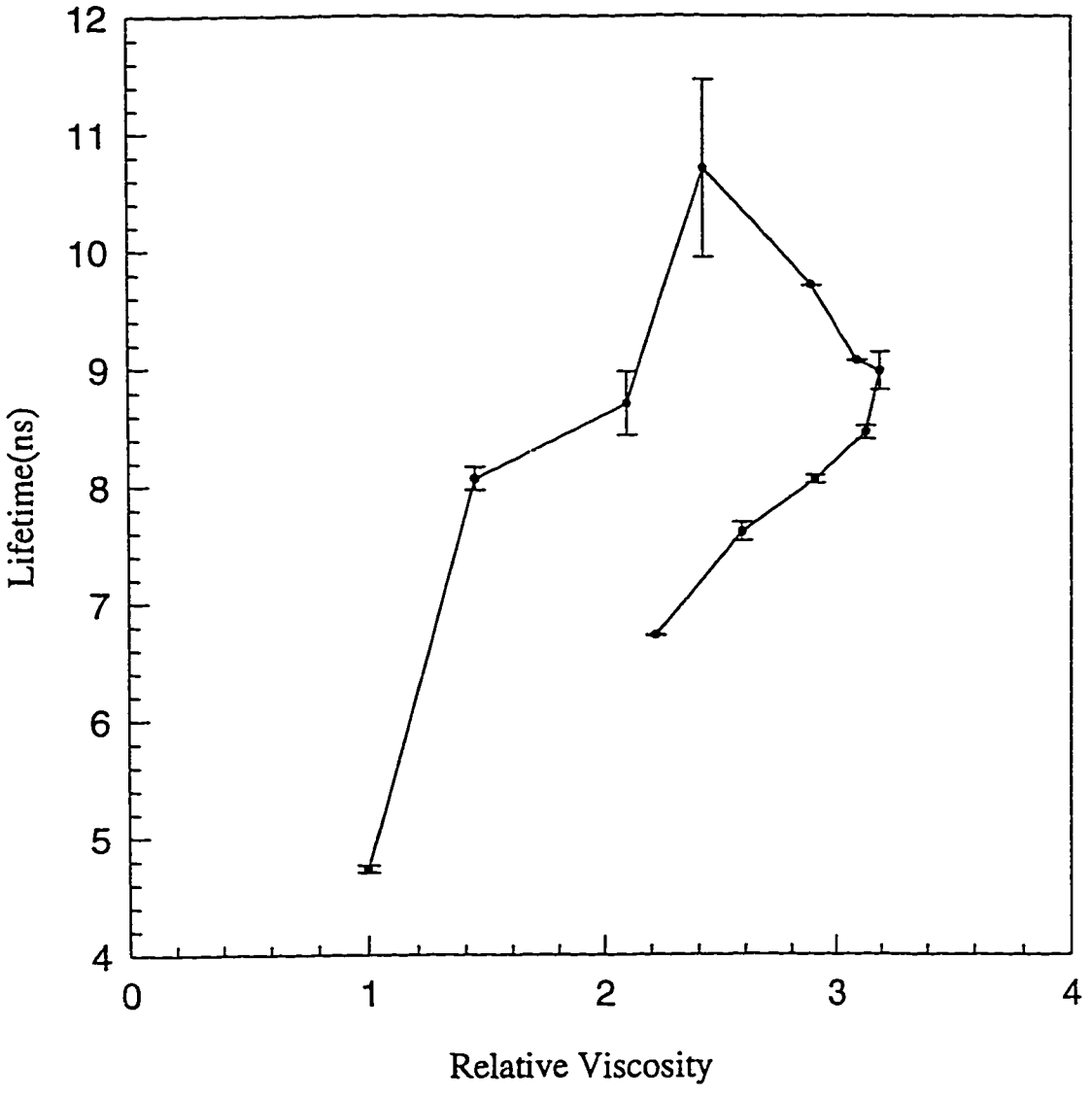

Figure 3.24: Correlation of the keto-enol lifetimes and the relative viscosities of 1-propanol-water mixtures at 400 nm emission wavelength.

3.4 Time-resolved Spectra of Thymine

In time-resolved spectroscopy, time evolution of the fluorescence is monitored at various time windows following the excitation pulse. In this particular case, excited state dynamics of thymine tautomers has been studied and the time-resolved experiment may be used for confirming the fluorescent tautomeric species.

3.4.1 Time-resolved Spectra of Thymine in Aqueous Solutions

The time-resolved spectra in the pH 2 and pH 9 solutions are shown in Figures 3.25 and 3.26 respectively. The time-resolved spectrum of thymine in pH 2 is similar to the time-resolved spectrum reported for 5-chlorouracil in an aqueous solution of pH 4[14]. A close examination of Figure 3.25 reveals that the band around 330 nm is intense at shorter times and weak at longer times while the intensity of the emission about 390 nm increases with time. Therefore, it is believed that fluorescence at shorter times of maximum about 330 nm arises from the diketo tautomer. On the other hand, longer time fluorescence with maximum around 390 nm is due to the keto-enol tautomer.

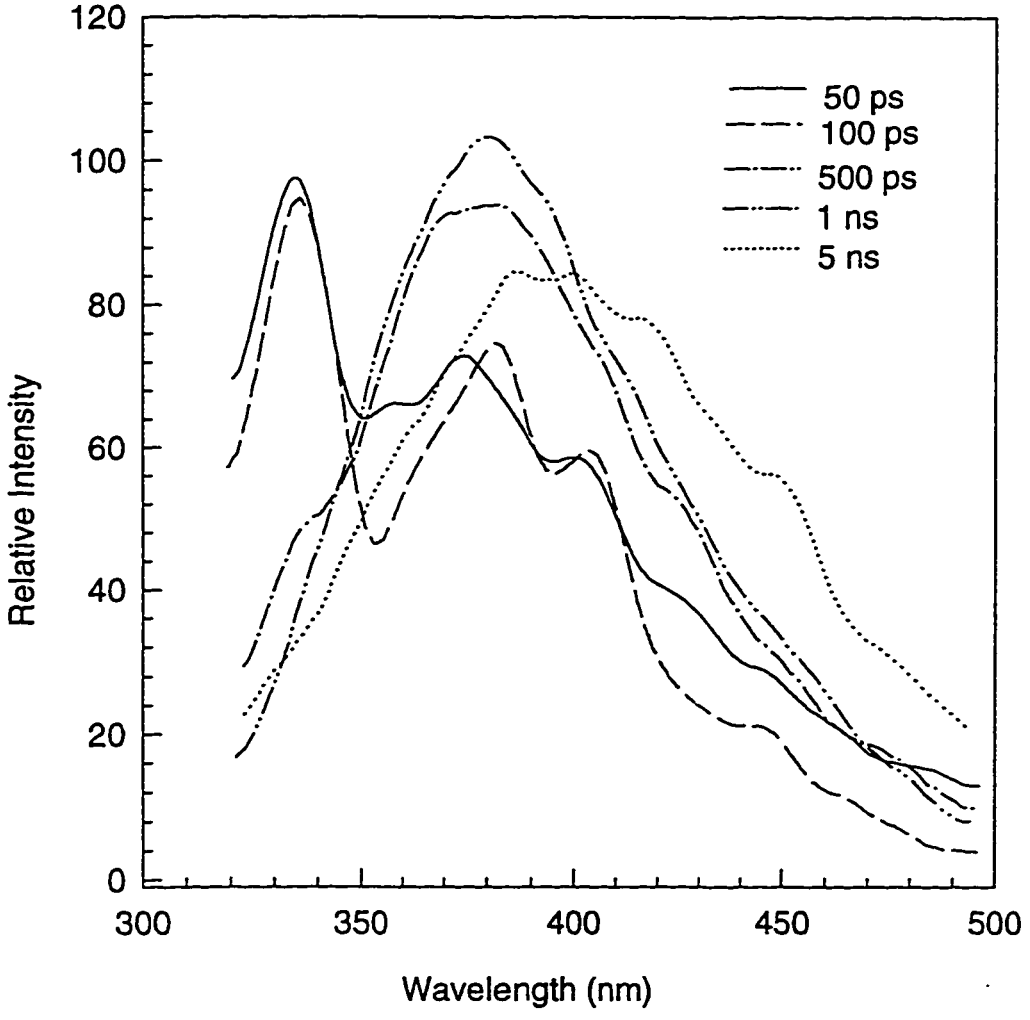

Figure 3.25: Time-resolved spectra of 10^{-4} M thymine in an aqueous soluton of pH 2.

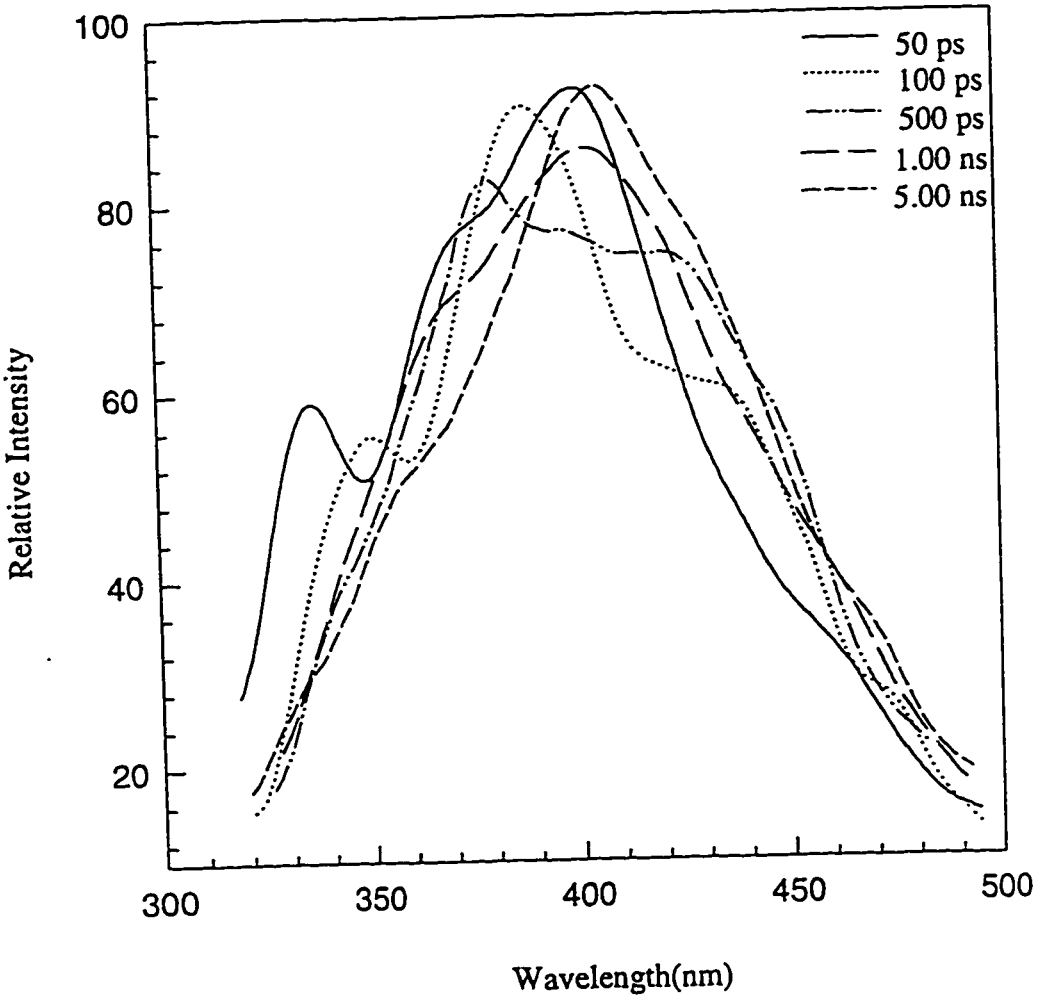

Figure 3.26: Time-resolved spectra of 10^{-4} M thymine in an aqueous solution of pH 9.

At this point, one has to address the question of Raman scattering interference where the band at 330 nm appears close to the Raman band observed in steady-state fluorescence spectra when the excitation wavelength is set at 295 nm. First of all, the band at 330 nm observed in the time-resolved disappeared when the time-resolved experiment was conducted for pH 12 solution, though the Raman band is evident in the steady-state fluorescence spectrum of the same sample. Moreover, this band is independent of excitation wavelength where it appears at the same position when the excitation is increased to 300 nm. Finally, the time-resolved experiment was run for neat water where a very weak band was observed at 330 nm believed to be due to thymine traces in the cell.

3.4.2 Time-resolved Spectra of Thymine in Various Alcohols and Alcohol-Water Mixtures

Time-resolved spectra of thymine in methanol ethanol and 1-propanol are shown in Figures 3.27, 3.28 and 3.29 respectively. Comparison of steady-state fluorescence spectra of thymine in water with the corresponding fluorescence spectra in methanol, ethanol and 1-propanol reveals that the fluorescence maximum in water is red shifted relative to alcohols especially when the excitation wavelength is set at the red-edge of the absorption band. As it was seen in the discussion of the steady-state fluorescence spectra in alcohols, the emission at 310 nm is attributed to the diketo tautomer.

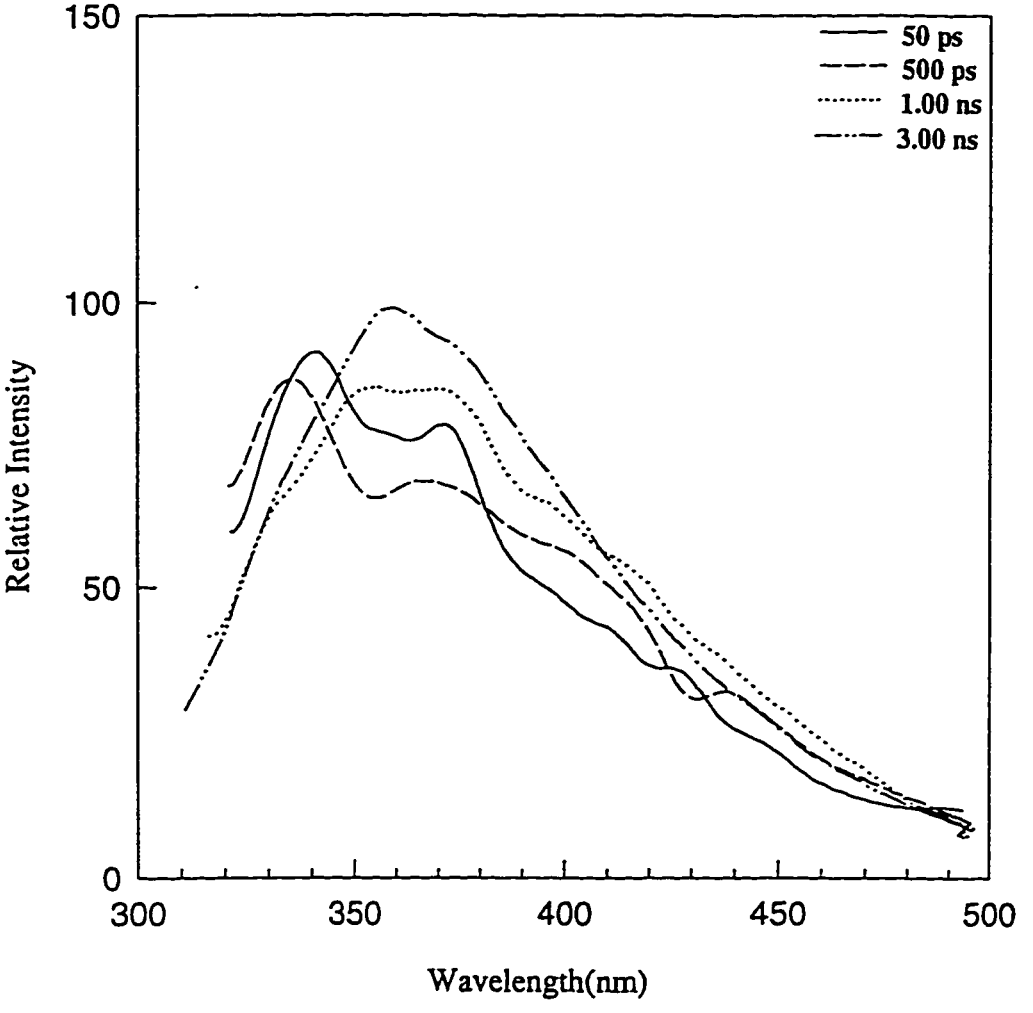

Figure 3.27: Time-resolved spectra of 10^{-4} M thymine in methanol.

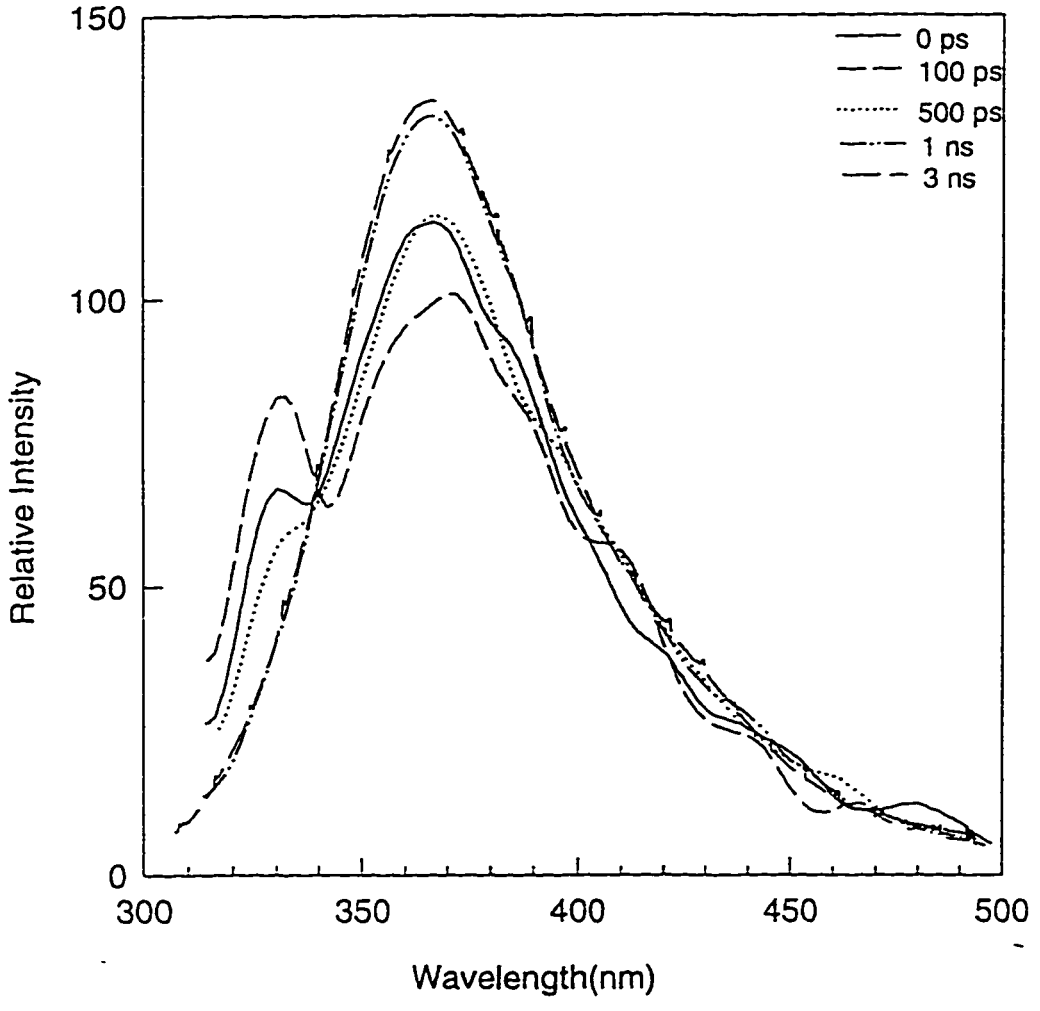

Figure 3.28: Time-resolved spectra of 10^{-4} M thymine in ethanol.

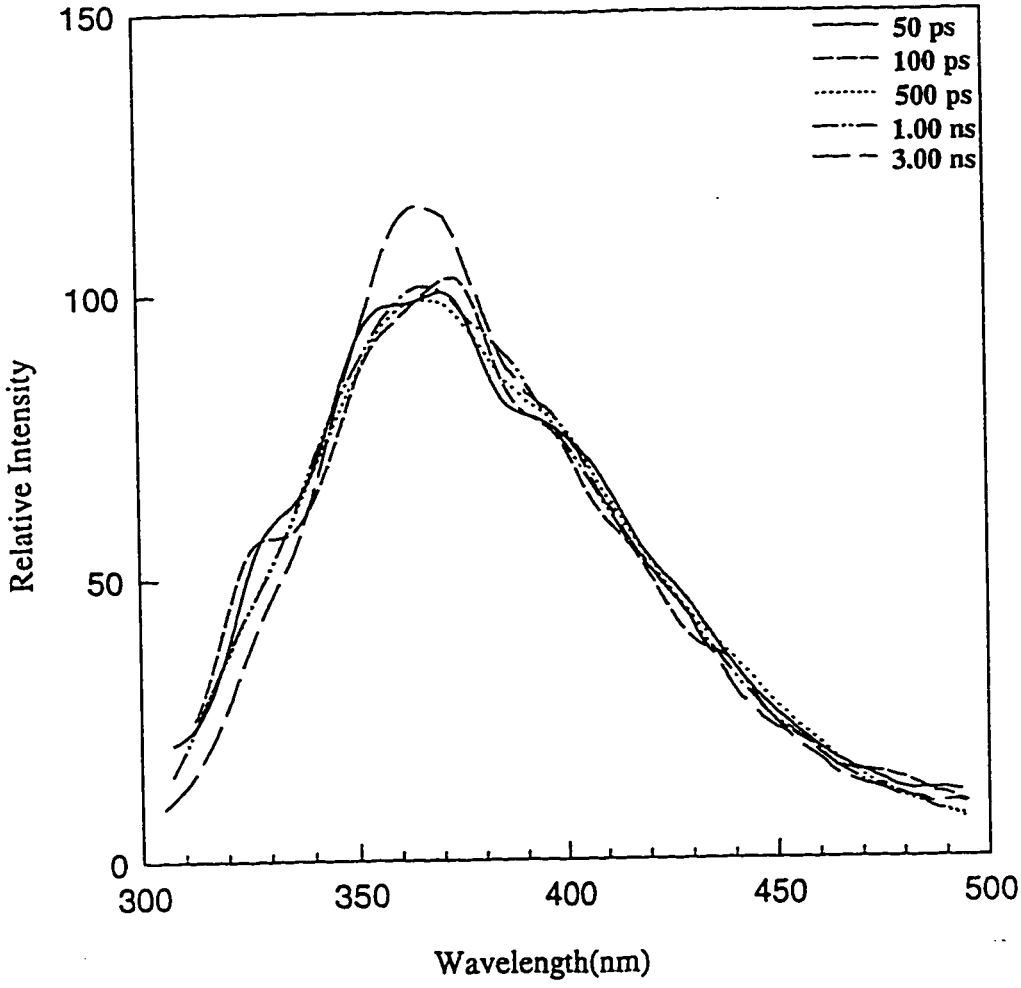

Figure 3.29: Time-resolved spectra of 10^{-4} M thymine in 1-propanol.

Accordingly, in the time-resolved spectra of thymine in alcohols, it is difficult to time-resolve the emission due to the diketo tautomer. This stems from the extensive overlap between the emission from the diketo tautomer with that of the keto-enol especially at the 360 nm band. Moreover, the weak emission of the diketo tautomer at 310 seen in steady-state fluorescence spectra is probably overlapped with the relatively strong emission at 325 nm at early times of the fluorescence.

To see the effect of water on the dynamics of thymine tautomers, time-resolved spectra of thymine in ethanol-water (7 : 3) and 1-propanol-water (7 : 3) mixtures have been collected as shown in Figures 3.30 and 3.31 respectively. Apart from slight decrease in quantum yield of the emission from the keto-enol tautomer no changes in the dynamics are observed.

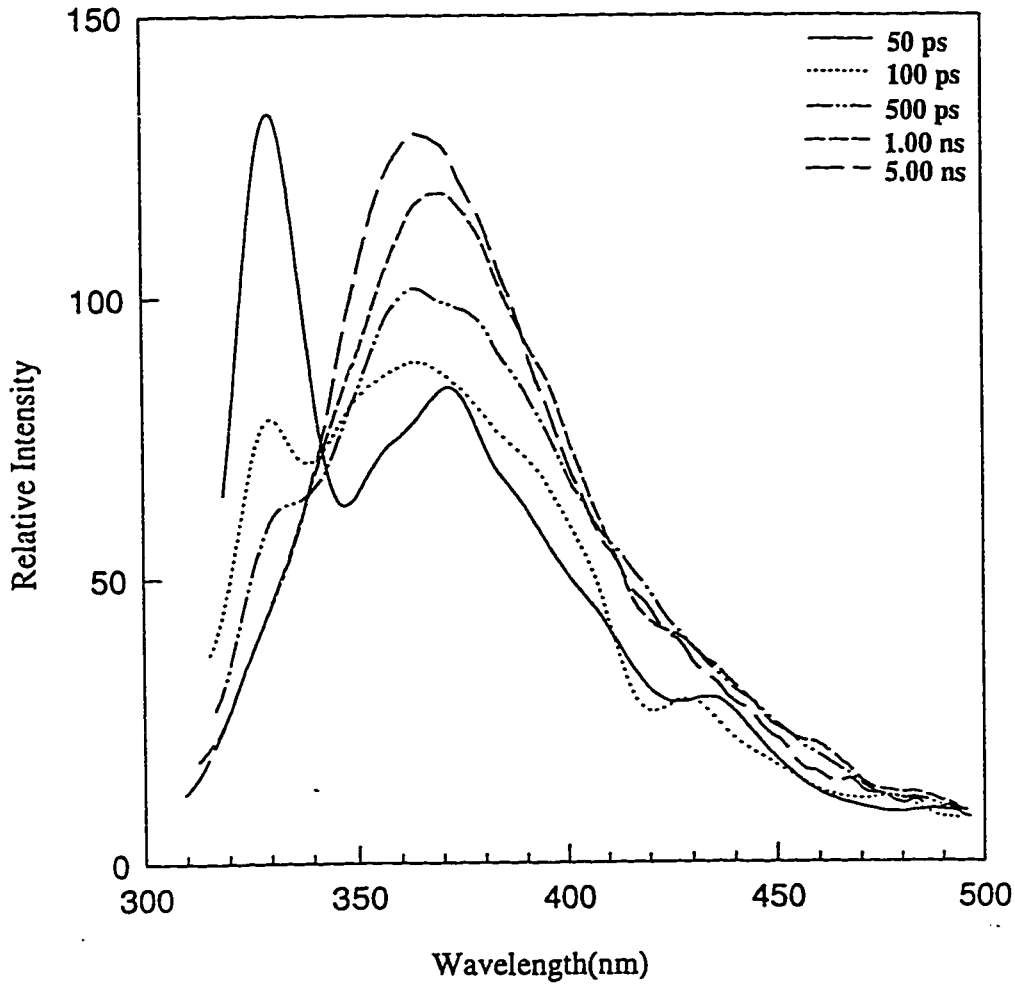

Figure 3.30: Time-resolved spectra of 10^{-4} M thymine in (7:3) ethanol-water mixture.

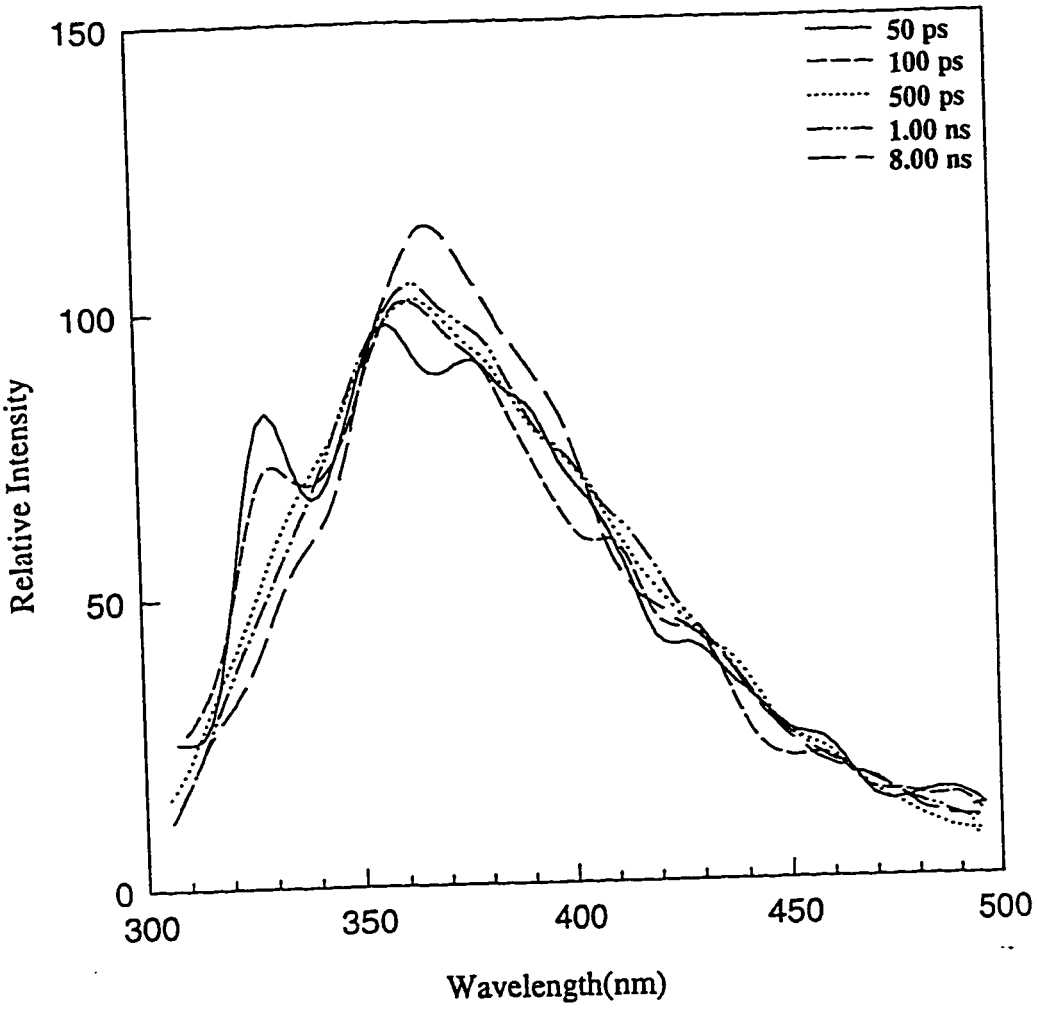

Figure 3.31: Time-resolved spectra of 10^{-4} M thymine in (7:3) 1-Propanol-water mixture.

CHAPTER IV

CONCLUSION

CHAPTER IV

CONCLUSION

The effect of pH and various alcohol-water mixtures on the electronic spectra and excited state dynamic of thymine have been investigated. Fluorescence spectra of thymine in aqueous solution where thymine exists in the neutral form have been found to vary in shape as the excitation wavelength is increased. Excitation at 260 nm gives rise to a fluorescence band with a maximum at 330 nm while excitation at 295 gives rise to another fluorescence band with a maximum of 390 nm. This phenomena is accompanied by an increase in the fluorescence intensity as the excitation wavelength is increased. This change in fluorescence shape as the excitation wavelength is varied is explained by the presence of another tautomer besides the predominant one. Based on the structures of thymine monoanionic tautomers and newly published theoretical calculations, it is believed that the keto-enol tautomer (II, Figure 1.1) is the minor tautomer besides, the diketo tautomer (I, Figure 1.1), the predominant species. Lifetime analysis of fluorescence decays of thymine support this explanation where a biexponential decay with lifetimes of around 0.7 and 4 ns is observed for the neutral form of thymine. The shorter and the longer lifetimes are ascribed to the

diketo and the keto-enol tautomers respectively. Time-resolved spectra of thymine are observed to be in accordance with this explanation.

Absorption spectra of thymine in the region 240-300 nm are found to be insensitive to the various combination of water, methanol, ethanol and 1-propanol mixtures.

Fluorescence lifetimes of thymine do not vary in methanol-water and ethanol-water mixtures while the lifetimes of the keto-enol tautomer is found to correlate with the relative viscosities of 1-propanol-water mixtures.

According to lifetime analysis and time-resolved spectra of thymine in various alcoholes-water mixtures, no pKa shift has been observed for thymine in the excited state.

REFERENCES

REFERENCES

1. Callis, P.R., Annu. Rev. Phys. Chem., 1983, 34, 329.

2. Hauswirth, W.W. and Daniels, M., Photochem Photobiol, 1971, 13, 157.

3. Wilson, R.W., Morgan, J.P. and Callis, P.R., Chem. Phys. Lett., 1975, 36, 618.

4. Vigny, P. and M. Duquesne, "Excited States of Biological Molecules", pp. 167-177, John Wiley.

5. Becker, R.S. and Kogan, G. Photochem. Photobiol., 1979, 31, 5.

6. Fujii, M., Tamura, T., Mikami, N. and Ito, M., Chem. Phys. Lett., 1986, 126, 583.

7. Baraldi, I., Bruni, M.C., Costi, M.P. and Pecprari, P., Photochem. Photobiol., 1990, 52, 361.

8. Morgan, J.P. and Daniels, M., J. Phys. Chem., 1982. 86, 4004.

9. Callis, P.R., Chem. Phys. Lett., 1979, 61, 563.

10. Williams, S.A., Renn, C.N. and Callis, P.R., J. Phys. Chem., 1987, 91, 2730.

11. Tsuchiya, Y.T., Tamura, T., Fujii, M. and Ito, M., J. Phys. Chem., 1988, 92, 1760.

12. Brady, B.B., Peteunu, K.A. and Levy, D.H., Chem. Phys. Lett., 1988, 147, 538.

13. Turpin, P. and Peticolas, W., J. Phys. Chem., 1985, 89, 5156.

14. Suwaiyan, A., Morsy, M.A. and Odah, K.A., Chem. Phys. Lett., 1995, 237, 349.

15. Lorentzon, J., Fulscher, M.P. and Roos, B., J. Am. Chem. Soc., 1995, 117, 9265,.

16. Baraldi, I., Bruni, M., Costi, M.P. and Pecorari, P., Photochem. Photobiol., 1990, 52, 361.

17. Petke, J.D., Maggiora, G.M. and Christoffersen, R., J. Phys. Chem., 1992, 96, 6992.

18. Callis, P.R., Photochem. Photobiol, 1986, 44, 315.

19. Ito, H., I'Haya, Y.J. Bull. Chem. Soc. Jpn., 1976, 49, 3466.

20. Danilov, V.I., Pechenaya, V.I. and Zheltovsky, N.Y., Int. J. Quantum Chem., 1980, 17, 307.

21. Eaton, W.A., and Lewis, J.P., J. Chem. Phys., 1970, 53, 2164.

22. Callis, P.R. and Simpson, W.T., J. Am. Chem. Soc., 1971, 92, 3593.

23. Lakowicz, J.R., "Principles of Fluorescence Spectroscopy," 1983, Plenum Press, New York.

24. Weber, G., "Fluorescence and Phosphorescence Analysis," 1966, John Wiley and Sons, New York.

25. Birch, D.J. and Imhof, R.E., Anal. Instrum, 1985, 14, 293.

26. Beechem, J.M., Ameloot, M. and Andre, J.C., Anal. Instrum, 1985, 14, 379.

27. Atkins, P.W., "Physical Chemistry," 4th Ed., Oxford University Press, 1990.

28. Green, R.B., J. Chem. Educ., 1977, 54, A365, A407.

30. Leven son, M.D., "Introduction to Nonlinear Laser Spectroscopy," Boston, Academic Press, 1988.

31. Fleming, G.R., "Chemical Applications of Ultrafast Spectroscopy," Oxford University Press, New York, 1986, Chap. 2.

32. Svelto, O., "Principles of Lasers," Plenum, New York, 1982.

33. Chan, C., Spectra-Physics Laser Technical Bulletin, 1979, 8, 1.

34. O'Connor, D. and Phillips, D., "Time-Correlated Single Photon Counting," Academic Press, 1984.

35. O'Connor, D. and Andre, J., J. Phys. Chem., 1979, 83, 1333.

36. MeKinnon, A., Szabo, A. and Miller, D.R., J. Phys. Chem., 1977, 81, 1564.

37. Shugar, D. and Fox, J., Biochem. et Biophys. Acta, 1852, 9, 199.

38. Ganguly, S. and Kundu, K., Can. J. Chem., 1994, 72, 1120.

39. Fox, J. and Wempen, I., "Advances in Carbohydrate Chemistry," Vol. 14, Academic Press, New York, 1959.

40. Nakanishi, K., Suzuki, N. and Yamazaki, F., Bull. Chem. Soc. JPN, 1961, 34, 53.

41. Wierzchowski, K., Litonska, E. and Shugar, D., J. Am. Chem. Soc., 1965, 87, 4621.

42. Berens, K. and Wierzchowski, L., Photochem. Photobiol., 1969, 9, 433.

43. Daniels, M., "Photochemistry and Photobiology of Nucleic Acids," Academic Press, New York, 1976.

44. Leszezynski, J., J. Phys. Chem., 1992, 96, 1649.

45. Weast, R.C., "CRC Handbook of Chemistry and Physics," 56th ed., CRC Press, 1975.

46. Gilbert, Andrew and Baggott, J., "Essentials of Molecular Photochemistry," CRC Press, 1991.

47. Beddard, G., Doust, T. and Hudales, J. Nature, 1981, 294, 145.